CUSTOMIZABLE TDI-BASED WHOLE BODY X-RAY SCANNER

by

Fevzi Aytaç Durmaz

B.S. ,in Electrical and Electronics Engineering, Bilkent University, 2007

M.S. ,in Biomedical Engineering, Boğaziçi University, 2010

Submitted to the Institute of Biomedical Engineering

in partial fulfillment of the requirements

for the degree of

Doctor

of

Philosophy

Boğaziçi University

2020

ACKNOWLEDGMENTS

I would like to thank all people who have helped and inspired me during my doctoral study.

I especially want to thank my advisor and mentor Prof. Dr. Cengizhan Öztürk, for his guidance during my research and study at Boğaziçi University. His perpetual energy in research and technology had motivated all his advisees including me. He provides me constant encouragement and a perfect balance between guidance and freedom throughout this study, and also the technology start-up idea.

I was delighted to be a part of X-Lab and BUMIL family. They made our lab a perfect place to work. I would like to thank especially my long-term colleague Altay BRUSAN, which helped me complete my PhD with his technical, as well as inspirational, support. I would also like to thank Alper Yaman, Murat Tümer, Asuman Kolbaşı ,and all my friends who are part of this long journey.

I would like to appreciate The Scientific and Technological Research Council of Turkey for supporting our projects under grant numbers 116E738, 116E879 , and Boğaziçi University Research Fund (BAP 6003).

My deepest gratitude goes to my family for their unflagging love and support throughout my life; this thesis is simply impossible without them. Thanks to my father Dr. Bilal Durmaz for his guidance and visions that he shared with me throughout his life. I am grateful to my mother for her devotions and kindness in my life. I feel proud with my sister Hande for her talents, I hope that she will be very happy, and my brother for being there with me when I needed.

ACADEMIC ETHICS AND INTEGRITY STATEMENT

I, F. Aytaç Durmaz, hereby certify that I am aware of the Academic Ethics and Integrity Policy issued by the Council of Higher Education YÖK and I fully acknowledge all the consequences due to its violation by plagiarism or any other way.

Name :

Signature:

Date:

ABSTRACT

CUSTOMIZABLE TDI-BASED WHOLE BODY X-RAY SCANNER

Medical X-ray systems are the gold standard in certain cases of medical diagnostics for over 100 years. The main scope of our studies is to develop a new full-body X-ray scanner device using line scanner detectors, and a plug and integrate hardware controlled system, this new device called SyncBox. Main focus of this particular dissertation is to control the total electronics and mechatronic systems of the device. full body X-ray scanner will be useful for trauma studies and bone surveys, where its high image resolution will help to identify more detailed images. SyncBox control system is a novel patented idea, that helps to integrate X-ray device components more easily and securely. Syncbox will help researchers to build up new, customizable devices faster, and it could begin a new developmental and even an industrial standard for X-ray imaging.

Keywords: Medical Imaging, Open Source Hardware, Medical Device Development, X-ray Applications, X-ray Imaging Hardware

ÖZET

ÖZELLEŞTİRİLEBİLİR, TDI TABANLI TÜM VÜCUT RÖNTGEN CİHAZI

Medikal görüntülemeye dayalı bazı teşhislerde x-ışınlı cihazlar 100 yıldan uzun bir süredir altın standart olma özelliğini sürdürmektedir. Bu tezin kapsamında çalışmalarımızın uzun vadeli hedefi, çizgisel dedektör kullanılarak yüksek çözünürlük tüm vücut görüntüleme yapma imkanı sağlayan bir cihaz geliştirilmesidir. Bu tezin kapsamı cihazın kontrol sistemi dahil olmak üzere tüm elektronik ve mekatronik kısımlarını içermektedir. Özellikle yoğun tarama amaçlı hızlı ve detaylı göüm vücut görüntüleme ihtiyacının olduğu travma gibi hastalıklara yönelik olarak tasarlanan bu cihazın x-ışınlı cihazlara yönelik farklı bir bakış açısı getire- ceği düşünülmektedir. Cihazın kontrol edilmesi için geliştirilen SyncBox kumanda modülü ile "tak çalıştır" şekilde direk röntgen cihazlarının geliştirilmesinin mümkün olabileceği bu tezde gösterilmektedir. Bu sayede araştırmacılara daha hızlı şekilde yeni röntgen cihazlarının geliştirilmesinin sağlanacağı ve sektöre bu doğrultuda yenilik ve geliştirme standartları getirebileceği düşünülmektedir.

Anahtar Sözcükler: Tıbbi Görüntüleme, Açık Kaynaklı Donanım, Tıbbi Cihaz Geliştirme, X-Işını Uygulamaları, X-Işını Görüntüleme Donanımları

TABLE OF CONTENTS

LIST OF FIGURES

LIST OF TABLES

1. INTRODUCTION

This dissertation is in the area of medical imaging, and more specifically in imaging hardware and software development for brand new X-ray medical imaging systems. In order to build a fully functioning X-ray device, the necessary hard- ware and image acquisition software components need to be brought together. Significant work are required on image quality, system optimization, preclinical, and early clinical testing. This study aims to accelerate the full development of a novel medical imaging device. This is a significant undertaking, but several earlier and still ongoing thesis work and ongoing research and entrepreneurial work have contributed to this endeavor[15, 16] . The critical software components of this final X-ray imaging device will be another Ph.D. thesis in parallel is presented elsewhere as a separate dissertation; (Development of a Modular Software Platform for Digital X-ray Systems with Time Delay Integration Scanner). Employment of time delay integration (TDI) detectors with fiber optics, and high-speed sensors, enabled to get faster acquisition on images with better quality. The novel components of this dissertation are to seamlessly integrate all necessary hardware for a new X-ray imaging device with more features than state-of-the-art. This novel device is destined to provide better image quality and more detailed anatomical information to the physicians.

1.1 Medical X-ray Devices

1.1.1 Physics of Radiography

The first medical X-ray image has been produced in 1985 by Wilhem Condrat Roentgen [17]. Figure 1.1 is the first X-ray image of a hand X-ray taken by him. His experiments with Crooke's tube has led to a new medical revolution towards the realization of several diagnostic and therapeutic devices over the next century [18]. First X-ray system in Turkey is used in military hospitals as shown in Figure 1.2 [1].

Figure 1.1 First X-ray picture of a hand. Taken 8 November 1895 by Wilhelm Conrad Roentgen, first presented in Würzburg Science Academy[1].

Figure 1.2 Left hand side is one of the first X-ray laboratory in Turkey, located in Yıldız Military Hospital, 1897. Right hand side is a X-ray process of a soldier with shrapnel wound on his hand, and his hand X-ray [1].

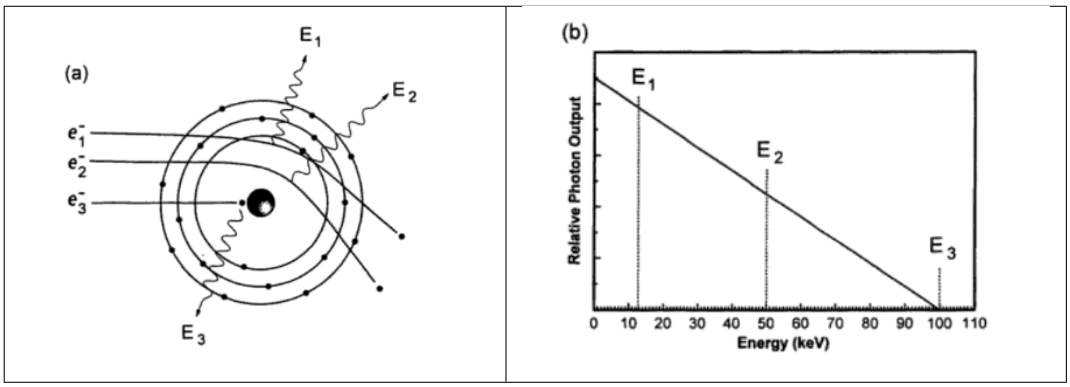

Figure 1.3 (a) Bremststrahlung radiation production with colliding the electrons with another metal and decelerated by the nuclei of the other atom. The energy on the electrons creates X-ray energy. (b) The probability of the X-ray production created by bremsstrahlung is dependent on the energy level of the electrons. Since there is statistically more energy production on low levels (E1), and higher energy levels (E3) are less [2].

X-rays are part of the electromagnetic spectrum. They interact with atoms depending on their high energy level [2]. 100 - 10 pm wavelengths are described as diagnostic X-ray in the EM spectrum [19]. X-ray beam acts like a hard stream moving at lightspeed. When X-ray photons collide with an atom, the orbital electrons eject from their orbits, and ionization occurs. This event is known as the photo-electric event. This physical phenomenon is the underlying principle for X-ray hard tissue imaging techniques. Another photon-atom interaction is called Compton scattering which is the scattering of a photon by an orbital electron. Since scattered photons have lower energies, it is commonly used in soft tissue imaging. [20],[17].

According to the bremsstrahlung radiation theory, if a charged particle is accelerated, it will radiate electromagnetic energy. When these highly energized electrons hit a metal target the velocity of the electrons change, and radiation occurs. Figure 1.3 shows electron interanctions with X-ray energy.

X-ray has several different interactions with the matter. These effects are generally described under different interaction types such as; photoelectric effect, Rayleigh scattering, Compton scattering, pair or triplet production.

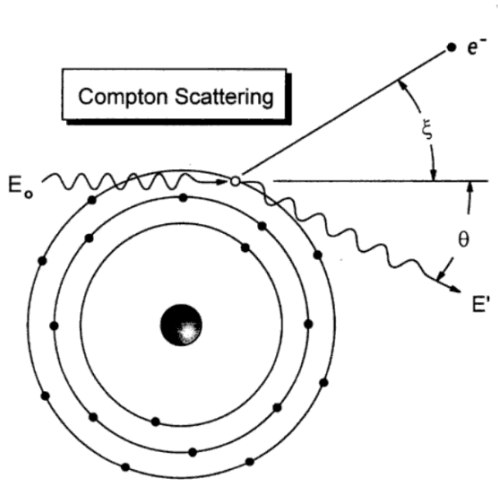

Figure 1.4 Compton scattering event. Some of the X-ray energy interact with the electrons on the outer shell. Electrons ejected from the outer shell and produce radiation. Scattered X-ray photon with reduced energy scatter from the atom [2].

1.1.1.1 Photoelectric effect:. The photoelectric effect is discovered by Albert Einstein in 1905 [21]. The energy of X-ray photons absorbed and transferred to the electron in the system. This process depends on the energy level of the X-ray which should be higher than the electron binding energy level. If the electrons are able to separate from the atom, they are bombarding to a target [20],[2].

1.1.1.2 Compton Scattering:. Compton scattering is discovered by A.H. Compton in 1923 [22]. The flexible collision of photons with the electron in the outer orbit of matter atoms is called Compton scattering. Energy and momentum are conserved in this collision in medium-energy gamma photons. Some of the incoming photon energy is given to the electron as kinetic energy. With the remaining energy, the photon deviates in terms of arrival and continues on its way. The high energy electron that occurs is called the Compton electron. Compton electron is absorbed in the material by ionization. Gamma photon, whose energy is decreasing, can make another Compton scattering or absorbed by photoelectric events. Figure 1.4. shows a compton scattering event [22].

1.1.1.3 Rayleigh Scattering: . In Rayleigh scattering, X-ray energy interacts with the electron and scattered as a result. Here the difference from the Compton scattering is that electrons stay at the orbit. Rayleigh scattering usually formed in low energy X-rays and does not produce ionization, and the energy of the scattered X-ray remains the same. Since the trajectory of the X-ray photons is changed, it creates a negative effect on medical imaging. Detection of the scattered X-rays are dispersed [23].

1.1.2 Projection Radiography

The intensity of the X-ray beam passes through the patient attenuates due to the interactions inside the body. Depending on the attenuating materials, photons which are passing through the body, reflect through a film or a digital detector.

1.1.3 X-Ray Parts

Medical x-ray systems consists of several parts and devices. Although we can directly project the X-ray on an imaging plate [8], the usage of indirect methods is a common technique which is converting the X-ray to visible energy spectrum and capture the fluorescent image for several technical concerns as DQE, SNR, noise, and cost [24, 25]. In this chapter instrumentationof the x-ray device explained and some x-ray parts will be introduced.

1.1.3.1 X-ray Tubes and Generators. X-ray radiography begins with the generation of a uniform X-ray beam. X-ray generator creates a high-voltage pulse to provide the necessary energy to create an X-ray beam. The generator consists of a high voltage power supply, a high voltage pulse generator, an impulse switching system with high-frequency control [18]. High-frequency generators can provide necessary tube current and required high voltage to X-ray tubes for X-ray production [26]. The

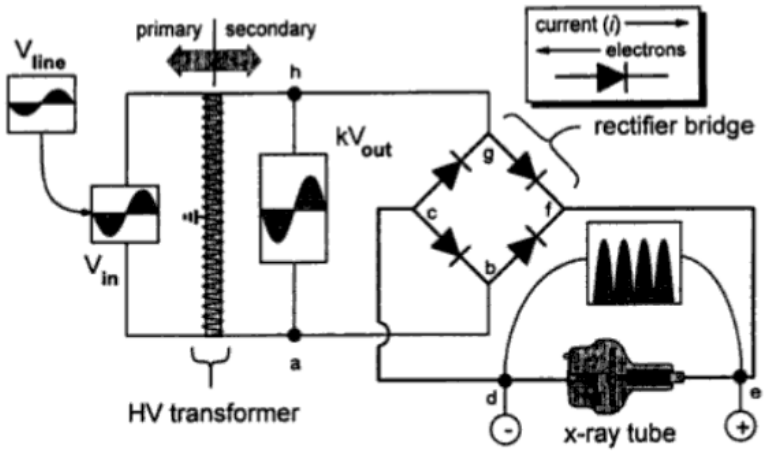

Figure 1.5 A circuit diagram for a single-phase high-frequency generator. A high voltage transformer creates a high voltage for the generator. The full-wave rectifier circuit creates positive cycles from the AC, and it generates a high voltage difference between anode and cathode of the X-ray tube [2].

general voltage interval for medical X-ray imaging is between 40 to 150 kVp. An X-ray generator is a form of regulated, pulse high voltage dc power supply. High-frequency generator can amplify the line voltage up to 200 kV, and current is usually between 1 to 5000 mA. The main advantage of the high-frequency generators is the production of low soft radiation which is useless for clinical use and hazardous for the patient. Most of the medical generators are between 35 kW to 100 kW. The voltage coming from the landline is increasing the voltage value up to 75 kV on the secondary side of the transformer. The full-bridge rectifier circuit converts the alternating current negative swings to positive creates a high potential difference waveform up to 150 kV. Figure 1.5 and Figure 1.6 are circuit diagram for X-ray production systems.

The X-ray tube is a vacuum tube that includes a filament and anode, which can produce ionizing radiation [27],[28]. The generator transmits the necessary voltage and current to the tube. Connecting a high voltage power source between anode and cathode creates a potential difference. The electrical field between electrodes speeds up the electrons towards the anode which is usually made with tungsten, molybdenum, or copper[29, 30, 31], and collision with the anode creates bremsstrahlung X-rays. An standard medical X-ray tube with rotary anode is shown in Figure 1.7.

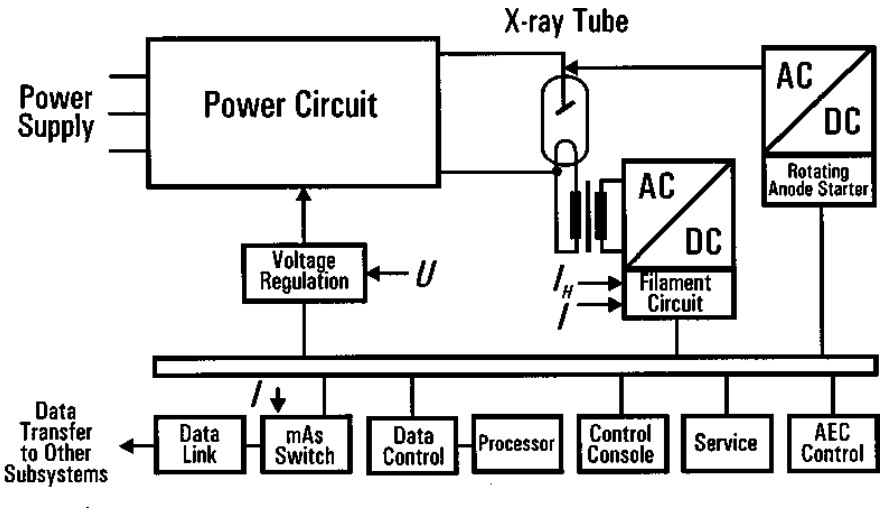

Figure 1.6 A block diagram for a processor-controlled X-ray generator [3].

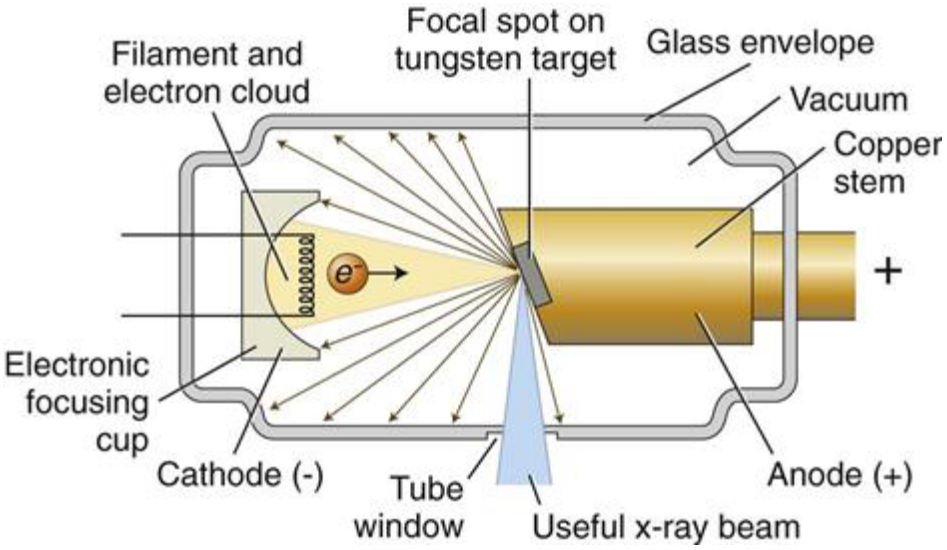

Figure 1.7 A conventional X-ray tube with tungsten anode [4].

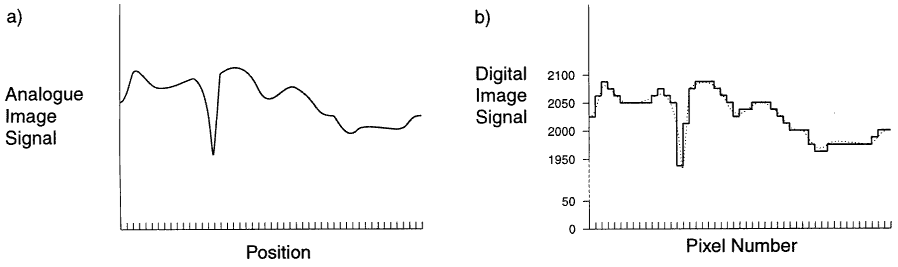

Figure 1.8 Digital Imaging vs Analog imaging. Analog imaging systems have a continuous signal, digital systems have discrete signals that needs to subsampled [5].

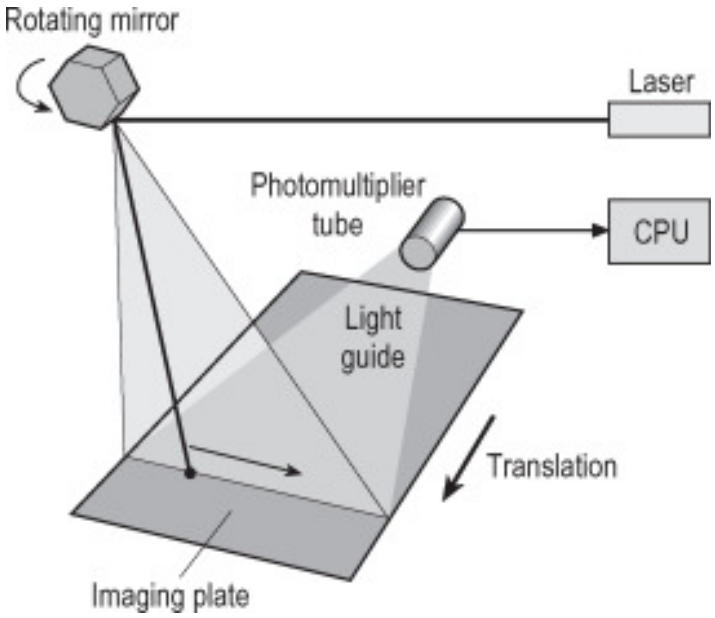

Figure 1.9 Computed radiography system image formation system [6].

1.1.3.2 Digital Radiography. X-ray detector is the equipment that captures the X-ray photons passes through the body [32]. The introduction of computed tomography (CT) in 1973 has also offered benefits of digital systems to the radiological systems [5]. Diagnostic systems able to transfer, display, and store in digital media and the ability to improve image quality [33].

Digital Imaging on direct radiography systems has been started with computed radiography systems [34]. It is an indirect X-ray image formation technique using cassette system with a photostimulable storage phosphor (PSP) screen plate. After PSP absorbs the X-ray exposure, a reader system scans the plate with a laser beam and record the data digitally [35]. CR systems have several advantages comparing to X-ray films such as dynamic contrast, digital data usage and storage.

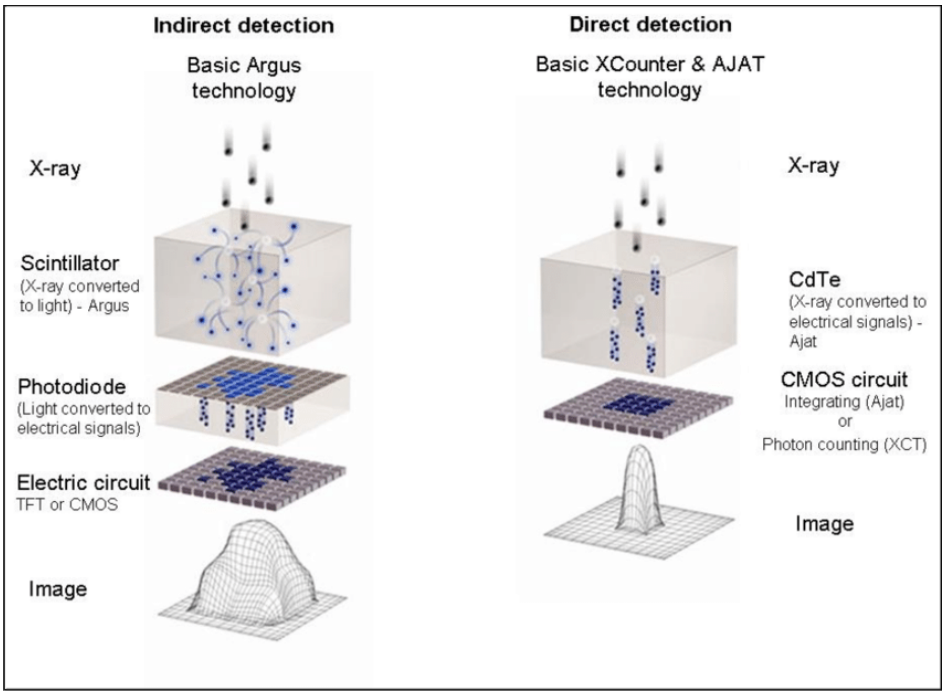

Figure 1.10 Direct and indirect X-ray detectors working principle [7].

Digital radiography systems are first fully digitized systems able to convert the X-ray photons to digital images without any further process. Two main working principles of DR systems are direct imaging and indirect imaging detectors. Direct imaging detectors use selenium based platforms. The most common used transistor is a selenium-coated thin film transistor (TFT) array. These array systems able to digitize the X-ray energy, and pass through a computer system. The indirect X-ray system working principle is to convert the X-ray photons to visible light and capture it digitally. These systems are based on thin films of silicon integrated with arrays of photodiodes. Photodiodes are coated with several alternative materials such as Cesium Iodide (CsI), Gadolinium dioxide, Sodium Iodine (NaI), or Bismuth Germanate (BGO).

CCD Based Digital Radiography Systems

Charged Coupled Device (CCD): previously revealed from flat panel systems they have a relatively older technology [36]. CCD systems use solid state electronics made of silicon crystals called (pixelated detector systems) it is an integrated circuit. Chips sizes are 0.2 -4.0 cm2 silicone in each structure. Photodiodes lined under the

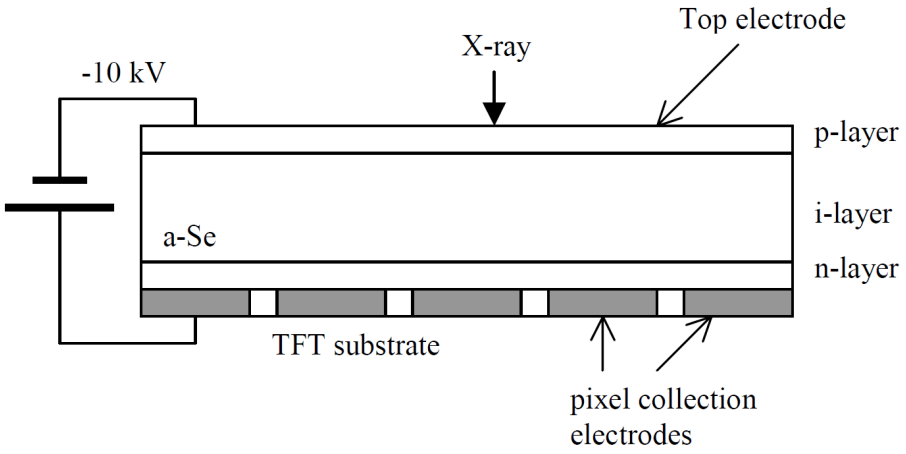

Figure 1.11 a-Se direct DR system cross section. X-ray photons generate electrons in the selenium middle layer. The accumulated charges are gathered by the bottom TFT layer, amplified and send to a computer system [8].

layer, independently of each other, called photosite or pixels. Pixel numbers on each CCD system could be upto 5 million on commercial products [36]. CCD systems have a wide area of usage for video cameras and digital cameras in industry and they are still widely used in digital fluoroscopy devices in radiology. X-ray CCD camera systems have a scintillator layer made of Gadolinium Oxisulfide or Terbium activated Cesium Iodide [37]. This layer is sort of phosphor crystal structure and falling on it It converts X-rays into visible light. After this process the rays are either passing through fiberoptic tubes or focusing with a lens is dropped onto the CCD chips, where they are converted into electrical signals. An analog to digital converter is used for digitizing the images [38]. Depending on the X-ray tube current applied during the exposure contrast has been arranged. After the radiation, the conversion of radiation to a visible light system stores the data in a matrix of photosites. The electrons accumulated do not go out. Then, with the voltage applied through the columns, the trapped electrons in each row at the same time moves to a lower rank. The bottom row every time electrons are digitized by an electronic process and an image is created from this data.

CMOS Based Digital Radiography Systems

Complementary metal-oxide semiconductur (CMOS) systems have been used in X-ray imaging for the last 20 years[39, 40] .CMOS is mainly a fabricated chip with a

pixel array design. Arrays are photosensitive transistors that forms a digital signal. Pixel size is usually around 120-200 microns. Although they have several advantages in digital imaging, CMOS systems creates higher electronic noise comparing to CCD systems. The system con-sists of a grid of phototransistors, covered with a material to transfer the X-ray into visible light, such as CsI or Gd2O2S. Since the system is using digital signals it has wider dynamic contrast and more adaptable to digital system usage [39, 40].

Other Digital Detector Technologies:

Direct Imaging: In com-parison to indirect devices, the energy converter and the final imager are the same part in a direct detector, for example an X-ray film strip is a material for direct detection. Because of its low absorption efficiency in the range of diagnostic X-ray energies, X-ray films require intensifying screens in medical imaging applications [27].

Direct X-ray detection is usually considered to consist of three processes: X-ray energy absorption, charge carrier generation (electron-hole pairs), and transportation of carriers to generate the signal. Due to its efficient absorption, high sensitivity, fast response and excellent energy resolution, direct X-ray semiconductor detector has become an attractive area of research in recent years. A technical comparison between direct and indirect X-ray detectors is shown in Figure 1.10.

Through the interaction of X-ray with semiconductor materials, pairs of electrons and holes are generated. A bias voltage is applied across the semiconductor which causes these charge carriers to move, leading to a signal [41].

A large international attempt has been done in recent years to develop a variety of semiconductor materials for X-ray and gamma ray detection systems with wide band gap and high atomic number. Among the semiconductor compounds, cadmium telluride (CdTe) and cadmium zinc telluride (CdZnTe) seem to be the most impressive radiation detector materials with high energy resolution, high detection efficiency and room temperature operation [42].

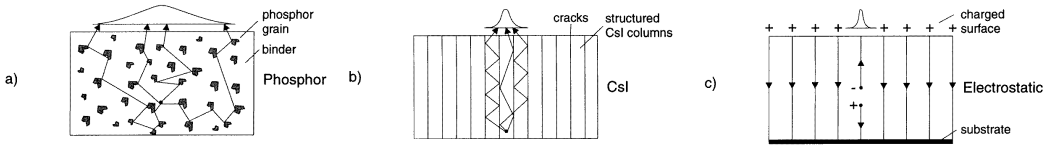

Figure 1.12 Three types of detector modalities. a) phospor systems for indirect imaging. b) CsI phosphor plate especially used in CMOS based digital indirect imaging systems, c) Direct X-ray imaging, X-ray creates a surface charge which converts to digital signals [5].

Another example in direct detection is, X-ray photoconductors such as amorphous selenium (a-Se) which could realize high-resolution imaging in mammography [43]. Nevertheless, the nearly-commercial a-Se direct X-ray imager has limited use because of its poor absorptivity of hard X-rays, low intrinsic X-ray sensitivity and insufficient charge transport ability. Therefore, the X-ray direct imaging is still developing on the way to mass marketing.

1.1.3.3 Control Units. The command console is the main control system of the device. All hardware will be connected to a computer system and controlled via software. The system will monitor the devices and uses interrupt signals to activate the system, X-ray exposure, image acquisition. The detector, generator, and movement control are provided through a PC controlled system. All electronic components such as the generator and detector will be controlled via this command console. The main aim is to design and develop an embedded system operating console to minimize the effects of operating system delays.

1.2 TDI Sensors

TDI (Time Delay and Integration) Sensors idea firstly developed during the 1970's. A multiline of CCD detectors sum up the intensity's during the procedure. By new technologic developments covering the TDI sensors with fiber optic, and CsI (Cesium Iodide) scintillator surface X-ray directly converts into visible photons and captured by the TDI camera. The main advantage of the TDI sensor is the speed and high resolution, regarding to other digital X-ray systems [5].

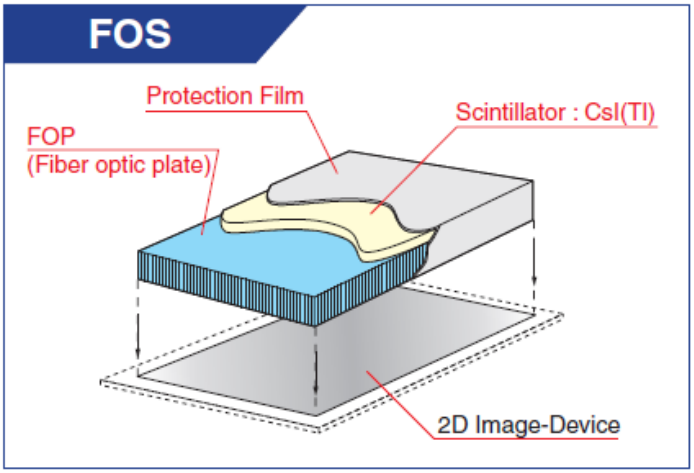

Figure 1.13 Layers of a TDI Sensor [9].

Fiber Optic scintillator covered TDI X-ray Camera system is a new approach to X-ray imaging. It is a useful product for in-line applications requiring high-speed operation with high sensitivity. Surfaces of the camera system can be seen over figure-1.13. Fiber Optic Surface (FOS) surface consists of three layers. The bottom layer is CCD plate, and over the top of the CCD plate there is a CsI scintilator for converting X-ray through visible light, and a Fiber optic plate (FOP) to converging the light intensity directly to the CCD without loss. FOP surface, and CsI coverage able to help system works with lower radiation and optimize the image resolution. During this dissertation we utilized TDI sensors. TDI sensors are able to provide higher resolution, and able to acquire all the body during a single scan. The main advantage of the TDI sensor is to acquire images constantly through a moving object. When the scanned object moves constantly, the signal is reinforced at each stage by integrating the signal. As a result of this protocol the system has able to make fast and sensitive scanning [44],[45].

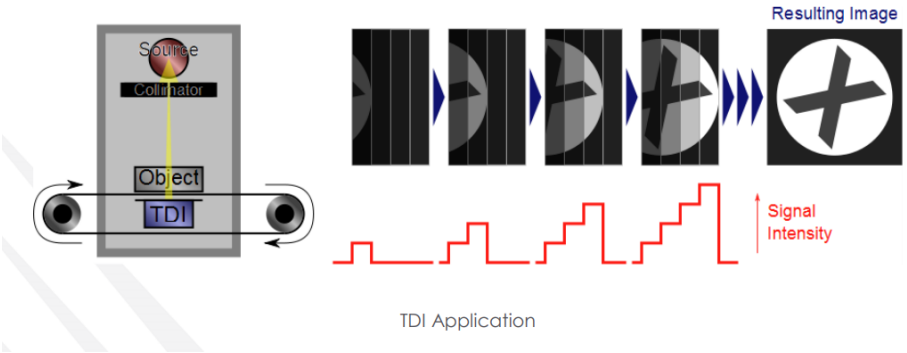

Figure 1.14 X-ray TDI workflow [10]. A moving object directly passes through the x-ray beam, TDI system captures section of the object and create and image formation. Combining several slices together increase signal intensity, and create a 2-D result image.

2. UNIFIED OPEN HARDWARE PLATFORM FOR DIGITAL X-RAY DEVICES; ITS CONCEPTUAL MODEL AND FIRST IMPLEMENTATION

2.1 Introduction

There are common underlying design principles and components in X-ray based projectional imaging modalities; such as chest radiography, linear and multi-directional tomography, mammography, bone density and skeletal radiography devices.

A standard X-ray device (Figure 2.1) includes a high frequency generator connected to a X-ray tube, a gantry area, a command console for exposure control and a detector for image acquisition [46]. In addition to these, there are several additional components frequently present in a medical X-ray imaging system: a motorized, fixed or mechanical collimator is used to navigate and narrow the beam of X-ray onto a target area; automatic exposure control (AEC) system to compensate the variations of the X-ray exposure towards the patient and maintain the image quality depending on the radiation levet coming throuh the detector, Dose Area Product (DAP) system to measure the radiation level exposed to the patient and a workstation to digitally control monitor and acquire the X-ray system [46 - 51]. Furthermore X-ray scanners employ various additional modules; there are collision and safety sen-sors, cooling systems, grids, electro-mechanical amd robotic instruments, security & interlock mechanisms and networking and storage capabilities [47, 48, 51, 52, 53]. Integrating all the above mentioned components is needed to a complete a radiography scanner.

Device vendors make a new radiography scanner by selecting the off-the-shelf components from different manufacturers based on the final device workload, budget and quality criteria and then introduce the combined system to the market. However, there is no accepted standard for component connectivity and communication, therefore the device integration process takes a considerable amount of time and effort. This

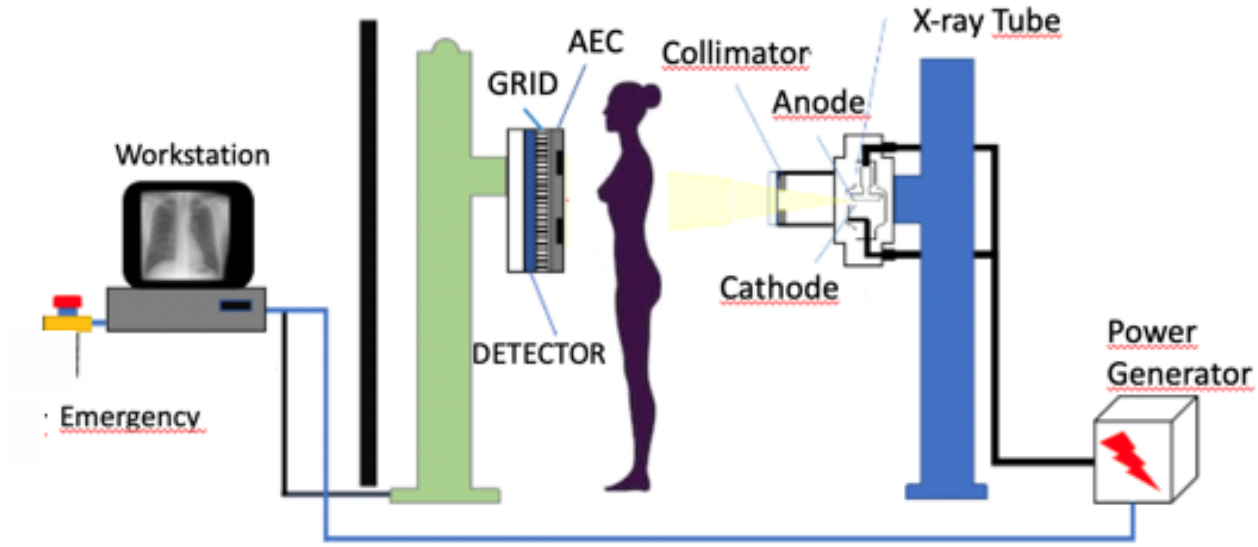

Figure 2.1 A general schematic of a tpical radiography scanner. High frequency generator produces the energy pulse and sends it through the X-ray tube. A collimator targets the X-ray beam over the target. Photons past through the subject and acquired by a detector. Digital image is transmitted to a dedicated workstation from the detector.

process often fails to eliminate all the uncertainties of the design; safety and efficiency issues are encountered during the clinical usage of these devices [54]. Imaging devices require a efficiency, safety and regulatory review whenever a component is replaced. Extensive device testing and calibration should be performed again costing significant time and money for each finite improvement.

On the other hand, researchers, who are interested in developing image processing and decision-making algorithms, face closed systems. In order to avoid risks, vendors restrict user access levels and hardware intervention capabilities. This conservative attitude limits the researchers to pre-configured options therefore making advanced research on these modern medical imaging devices very challenging.

Complementing open platform-based trends in medical device development, we introduce here a conceptual model for digital X-ray scanners and introduce an open source hardware device and platform, named 'SyncBox'. This platform employs Plug-Integrate-Play (PIP) manufacturing paradigm to the X-ray radiography device design

and introduces a potential solution for its integrability and extensibility problems.

In the following parts of this paper, the background of Plug and Play (PnP) in medicine is discussed next. Methodology Section discusses the X-ray device model and introduces the SyncBox concept in detail. Results Section describes the first implementation of this platform to develop a special time-delay integration scanner. It is followed with the discussion of these discusses the initial results, its current limitations and how these systems could be improved. Potential impact of this device on medical industry discussed in the Conclusion Section.

2.2 Background

Healthcare delivery organizations are starting to view the interoperability gap as a real problem: a barrier to innovations that could potentially improve patient safety and health care affordability [55]. Medical device interoperability is the ability of medical devices, clinical frameworks, or their related systems to communicate with each other in order to safely fulfill an intended purpose [56]. Effective interoperable medical systems should be safe, secure and usable at all levels of conjunction and require holistic view [57]. Tolk et al. postulated a model consisting of five levels for conceptual interoperability [58], which was then extended to seven levels by Turnitsa et al. [59]. These models characterize the internal and external interactions occurring in systems. Robkin et al. [60] extended these models for medical devices and health care systems.

The standardization bodies, consortium of manufacturers and academic researchers have been leading an extensive effort to make medical systems interoperable and to create a complete Plug and Play (PnP) system structure [61],[62]. The "Med-ical Device Plug-and-Play Interoperability program" was founded in the US [62] to develop an open-source clinical environment (OpenICE) [63]. The MD PnP Lab [62] was opened in May 2006 to provide an environment to support projects, testing and prototyping of a vendor-neutral "sandbox" solution [62]. In Germany flagship project

OR.NET [64] focused on secure and dynamic interlinkage of medical devices in the operating room and hospital.

Regulatory bodies also have made great contributions on defining the standards. As a context in ISO/IEEE 11073 “Health Informatics - Medical / Health Device Communication Standards”, a set of standards was designed for enabling communication between medical, health care and wellness devices and with external computers [65]. Moreover, the ASTM F2671 “Essential Safety Requirements for Equipment Comprising the Patient-Centric Integrated Clinical Environment (ICE)” [66], is a series of standards that conceptualize excellence in biomedical and health system design and development practices [67, 68].

Association for the Advancement of Medical Instrumentation (AAMI) adopted an interoperability hierarchy model based on Turnitsa model [69] (Table 1). In this model, Level 0 interoperability describes a situation in which two systems have no need to, or cannot, interoperate and the interoperability is accomplished by hand. Technical interoperability (Level 1) is accomplished when two frameworks have the way to impart yet neither has a common comprehension of the structure nor the significance of the information being connected. In this level, a stream of bits or bytes could be sent between the systems, however, none of the sides has the facility to interpret the data. Syntactic interoperability (Level 2) occurs when information is communicated with structure but without any meaning. In other words, in this level, both sides know the data format but received data makes no sense.Semantic interoperability (Level 3) is accomplished when the information is valid and operative, however a full comprehension of the connections between components of the information and the setting of the information is absent.Ideally logical interoperability (Level 4) incorporates a mutual comprehension of the information, the connections between components of the information and the setting of the information. In any case, down to earth interoperability can’t oblige changing connections or setting. Dynamic interoperability (Level 5) is increasingly adaptable, taking into consideration changing settings and connections after some time or inside the extent of explicit exchanges [69] .

Table 2.1
Levels of interoperability: Different levels of interoperability abilities from 0 (no interoperability) to 5 (dynamic interoperability) [69].

	Level	Name	Description	Standart
Inter-operability	5	Dynamic	Components' internal states and capabilities understood	None
	4	Pragmatic	Context understood	IHE PCD Continua
Integrability	3	Semantic	Meaning understood	SNOMED Continua/ 11073 Nomencla-ture IHE-PCD/ 11073 Nomenclature
	2	Syntactic	Common format	HL7 11073 series
Connectivity	1	Technical	Common physical and transport	Ethernet, WiFi, USB
	0	None	None	

In order to solidify the foundation for a safe, secure and reliable device interoperability, device models have been used. A device model consists of the device context and dynamics. Main purpose of the device model is to support the system designer to build up a safe device design for both machine operator and patients [54],[70]. A device model is usually prepared from different views (e.g. data, dynamics, run-time) and depends on the level of interoperability presented in Table 1; it may contain details such as data encoding format (e.g. float type format), units of measurements (e.g. mmHg, beats/min) and measured parameter (e.g. blood pressure, O2 concentration). ASTM F2761-Medical Devices and Medical Systems Essential Safety Requirements for Equipment Comprising the Patient-Centric Integrated Clinical Environment (ICE) proposes the following principles to increase the safety and security of connections: a The connected equipment does not fail due to receipt of messages or other information. b Failures caused by direct or indirect connection to an interoperable component, electrical and logical mismatching, erroneous commands, receiving and processing erroneous data or commands, or not adhering to the non-functional requirements of the communication specification, should be considered in verification of the system[66].

The mature form of interoperability is Plug-and-Play (PnP). At this level, devices interoperate with each other seamlessly and solely based on configuration without significant engineering effort [58, 59, 60]. PnP capability could bring great reductions to the burden of patients, physicians and hospitals and it could prevent technical issues and clinical workflow inefficiencies by integrating the data and functionalities of medical devices and clinical information systems [55]. However, a complete PnP implementation is difficult and it requires a multi-layer device model. Device model includes a service model, data format, process, communication protocols depending on the standards [65, 71], control and management properties [60, 72].

In the next section a device model for digital X-ray scanner is introduced. This model is then applied for developing a unified open source hardware platform.

2.3 Methodology

A plug-integrate-play (PIP) for X-ray imaging system is introduced here as an open hardware platform; our solution, SyncBox, aims to bring Level-4 interoperability to the radiography devices. SyncBox has designed with central hub architecture (Figure 2.2); various compulsory (e.g. detector, high frequency generator, X-ray tube) and additional units (e.g. AEC, robotic movement, DAP, cooling system) utilized in a medical and industrial radiography device (e.g. non-destructive X-ray quality control systems, security X-ray machines) are all connected to this central SyncBox in a star network structure. As a result, all the communications between devices are accomplished through the SyncBox and none of the components is connected to others directly. SyncBox is responsible for providing communication channels between units, translating connection protocols, handling communication standards, managing system-level workflows, message translation and monitoring the overall device security and safety.

Technical and syntactic integrabilities (Level-1 and Level-2 in Table 1) and semantic interoperability (Level 3 in Table 1) for X-ray scanners are mostly related to the controlling and signal handling of the components. Following the ASTM F2761 guidelines, the SyncBox is required to provide isolated and reliable channels between itself and each device. The pragmatic (Level-4) and dynamic (Level-5) interoperability involves more sophisticated problems and usually includes more computationally intensive operations and entangled system workflows between the X-ray scanner and the peripheral devices, such as the archiving systems. Hence, the communications and workflows categorized in various ways: low speed or high-speed data transfer and/or process control. Each category requires different computational capacity and could be implemented differently. At Level-1 up to Level-3, interoperability is achieved via a micro-controller, while Level-4 and Level-5 require a more sophisticated computer such as a mini-computer (also known as Computer on Module - COM).

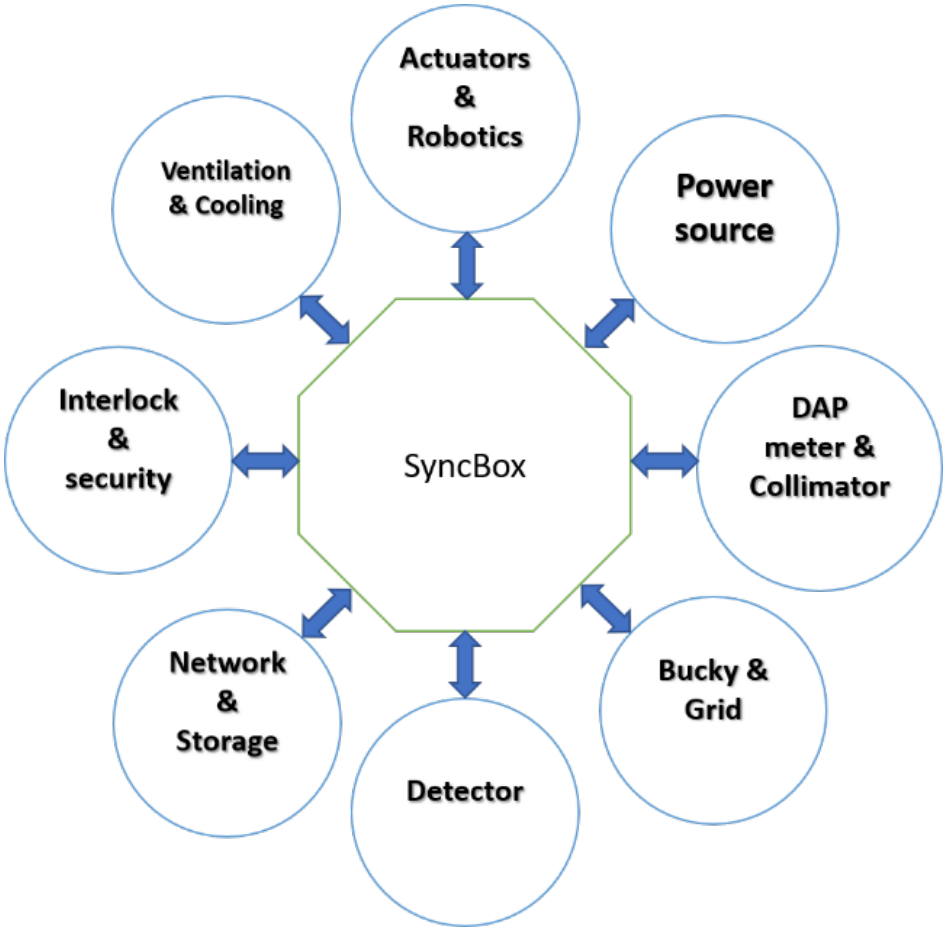

Figure 2.2 The central hub architecture. SyncBox is placed at the heart of an X-ray scanner. All components are connected to the SyncBox and all communications and transactions are accomplished through it.

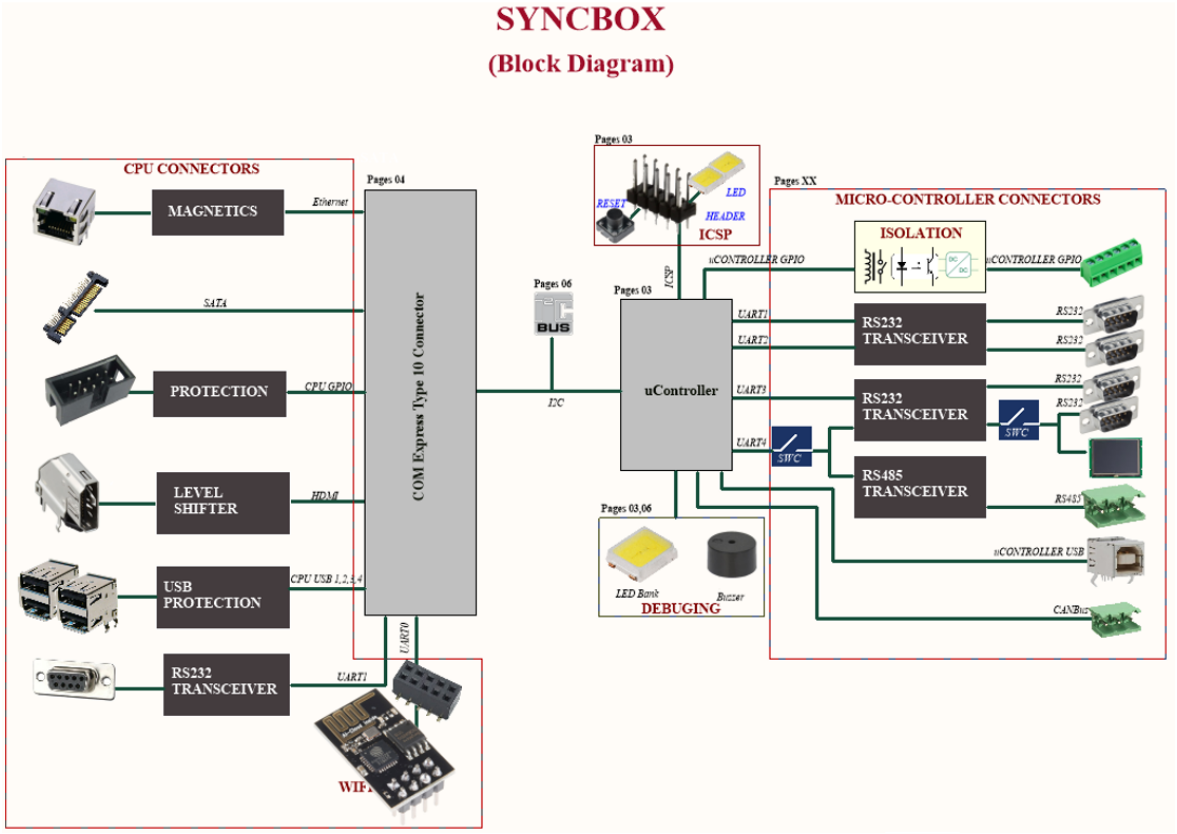

Figure 2.3 SyncBox Block Diagram with CPU and microcontroller based connections. MicroProcessor Controlled Units and connections are used for advanced operations such as image acquisition, post processing, network based communication and user interface. Microcontroller Controlled Units and connections are responsible for fast and reliable communications: X-ray exposure control, emergencyand safety sensors, mechanical driver communications.

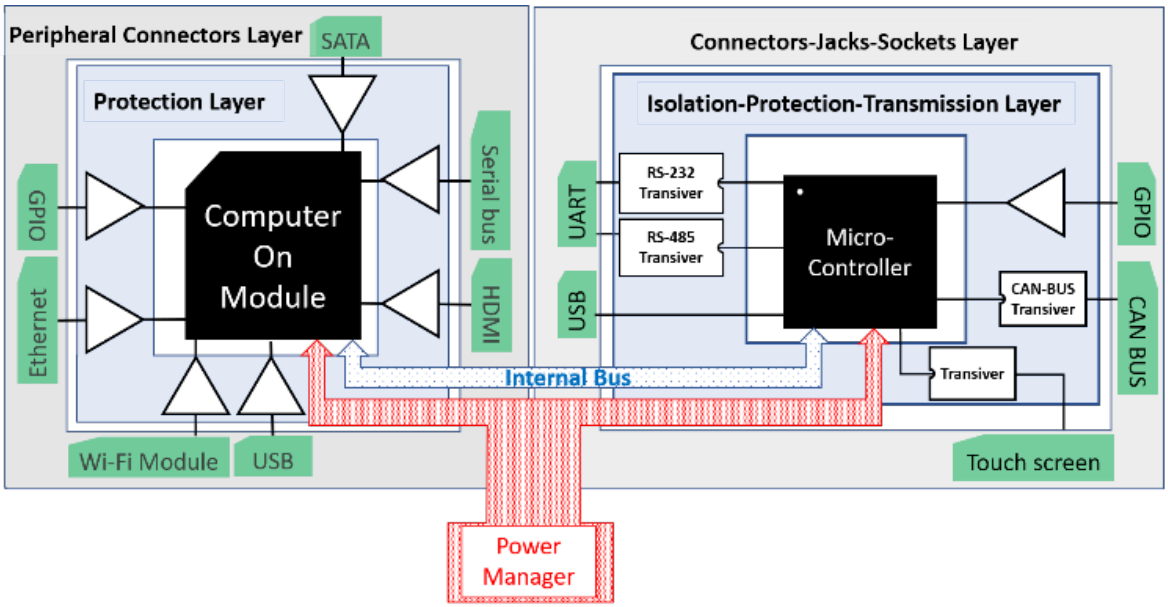

Figure 2.4 Abstract schematic hardware architecture. Each component of X-ray device (Figure 2.2) is connected to one of the peripheral connectors.

2.3.1 Hardware Schematics of SyncBox

SyncBox is a combination of a two level hardware: a microcontroller based system and a microprocessor based platform. Microprocessor controls advanced operations and workflows such as image acquisition, task organization and interacting with users. Microcontroller system controls the low level operations such as device controls, X-ray control and exposure, sensors. SyncBox block diagram showed on Figure 2.3 including the CPU and Micro-controller based connectors. The hardware organization schematic of SyncBox implementation is shown at Figure 2.4. The Hardware Application Layer (HAL) executes within the micro-controller (Figure 2.6).

The microcontroller and microprocessor are connected to each other over an internal bus and the power manager circuit provides the required powers to all sections, as shown in Figure 2.4. The protection layer provides a shielding against ESD and cable discharge event (CDE). The medical standards require circuit protection against electrostatic discharge (ESD), Electromagnetic interference (EMI) and wrong cable plugs. To protect against these disruption sources, all communication headers and junctions are passed through a layer of protection and denoising and then connected to

a microcontroller. Some protocols, such as CAN bus and RS-485, also require a special transceiver module. These modules also provide a level of protection against voltage shocks. Finally, the general-purpose input output (GPIO) provides the extension paths for systems with unknown requirements.

2.3.2 Dynamic Model of SyncBox

The dynamic model of SyncBox, as shown in Figure 2.6, is applicable to most of the radiography devices, with minor adjustments. A typical workflow is given below.

- Initially, user defines a set of exposure parameters, such as X-ray energy, intensity and duration, to the SyncBox. This interaction between the user and SyncBox is accomplished via SyncBox's mini-computer or touchscreen display.
- After getting the user confirmation, SyncBox micro-controller is informed with the imaging tasks.

From this step onward, it is the responsibility of the micro controller unit to handle the interoperability between the devices and orchestrate the ensuing image acquisition.

- It first prepares all the required devices (such as detector, generator, mechatronics or any other device), then starts the examination.
- After all previous programmed steps are accomplished succesfully, the captured image is grabbed by the mini-computer and displayed to the user; otherwise, error recovery mechanism is initiated.

The type and the content of the messages, signals and acknowledgments that is sent to each device is different. Each manufacturer provides a set of instruction guides for their product to describe how to communicate with their components. Besides this, some devices may require communicating with the others directly. In the following

Table 2.2
SyncBox Sections. This table shows all main sections included in SyncBox. System includes I/O ports, power circuit design, a microcontroller, a micropc, display and storage units.

Section	Title	Details
a	RS-485	Full duplex protocol
b	CAN bus	Three pins header
c	GPIO	Single and paired GPIO
d	RS232	No parity, no handshaking, 8-bit
e	PIC24EP512GU810	16-bit micro controller
f	Isolation and protection	Input direction, output direction and Input-Output direction
g	Transceiver	Serial bus connectors
h	Transceiver	High speed connectors
i	in-circuit serial programming (ICSP)	Upgrade microcontroller firmware
j	COMe Type 10 mini	Intel Celeron with 4 GB RAM
k	Ethernet	Gigabit ethernet
l	USB II and III	Connected to COMe
m	HDMI	COMe display out
n	GPIO	Connected to COMe
o	Wi-Fi socket	ESP8266 Wi-Fi Module
p	Touch screen socket	Microcontroller connector
q	SATA	External hard disk
r	Power manager	12V input to +5 and +3.3

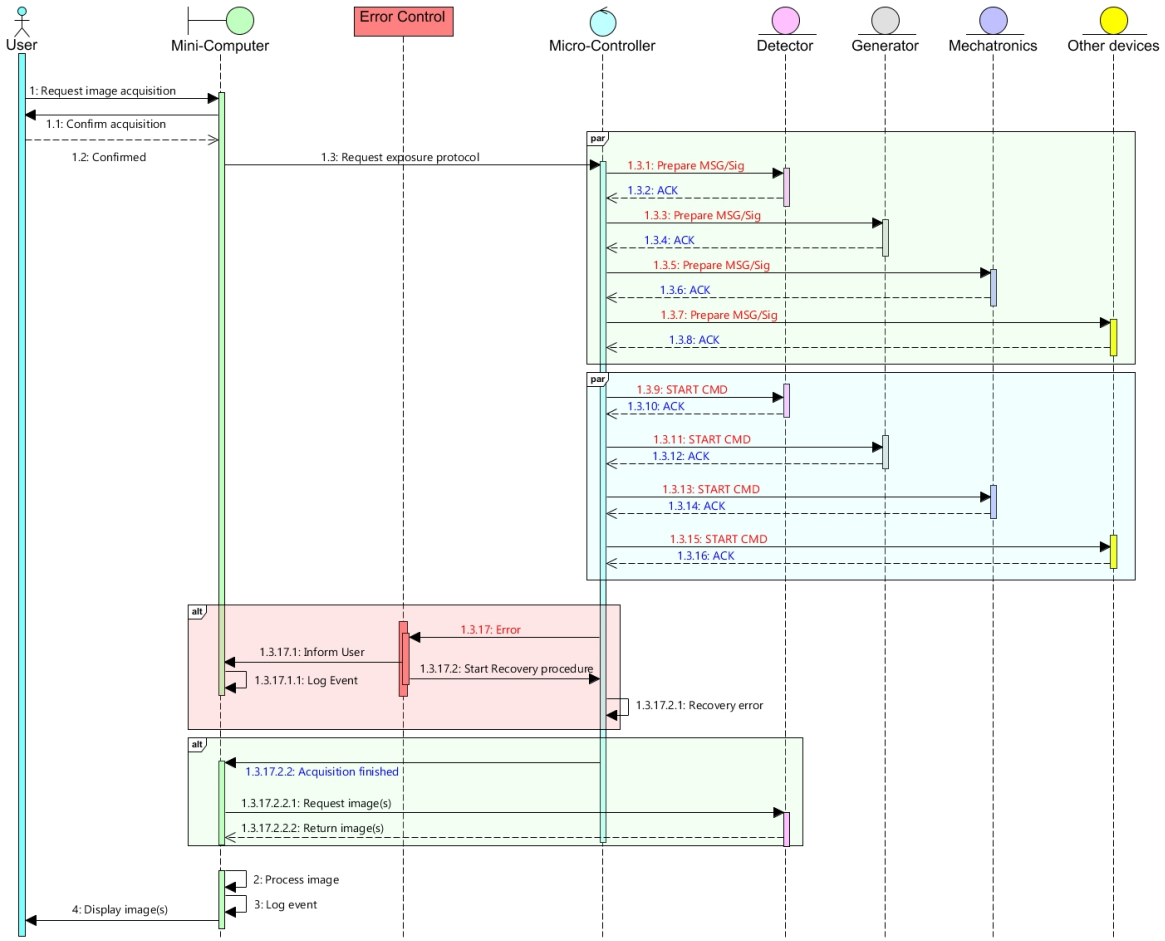

Figure 2.5 Data model of SyncBox. Transactions are divided into low speed and high speed. Each category is implemented by a special device. A simple work flow diagram for a X-ray protocol.

section, we will discuss how the SyncBox software and hardware architecture is designed to handle all these requirements.

The extended processing tier (as displayed in the top section of Figure 2.6) executes on a computer-on-module express (COMe) unit.

2.3.3 SyncBox Software Architecture Model

SyncBox software architecture is shown in Figure 2.5. The hub has a two-tier-architecture: the Hardware Abstraction Layer (HAL), which is executed on micro-controller and the Extended Processing (EP) layer for high-level interoperability tasks run on the mini-computer. The HAL provides the technical, syntactic and semantic interoperation services. EP layer provides a context for data processing and systemic extension ports (Level-4 and Layer-5 in Table 1).

In this architecture, it is assumed that non-trivial peripheral devices (e.g. power generator) have a firmware (or a feedback circuitry) with the internal data and state variables and expose a set of functionalities, known as Application Programming Interface (API), to the outside world. Clients connect to the device through a physical interface and exploit these public APIs. Normally, these API functions accept streams of bits (or bytes) as inputs and produce streams of bits as outputs. However, edge or pulse signals are not uncommon in old devices.

In the core of the HAL, there exists a small piece of code, kernel, which is responsible for fundamental operations. It accepts the messages as a stream of bits, then encapsulate and put them into appropriate memory locations. As a result, it avoids message loss that may occur due to the load of simultaneous flow of incoming messages. One could imagine that the kernel is a virtual secretary that receives a set of unordered papers from different senders, organizes all these incoming papers and places them within appropriate folders [14].

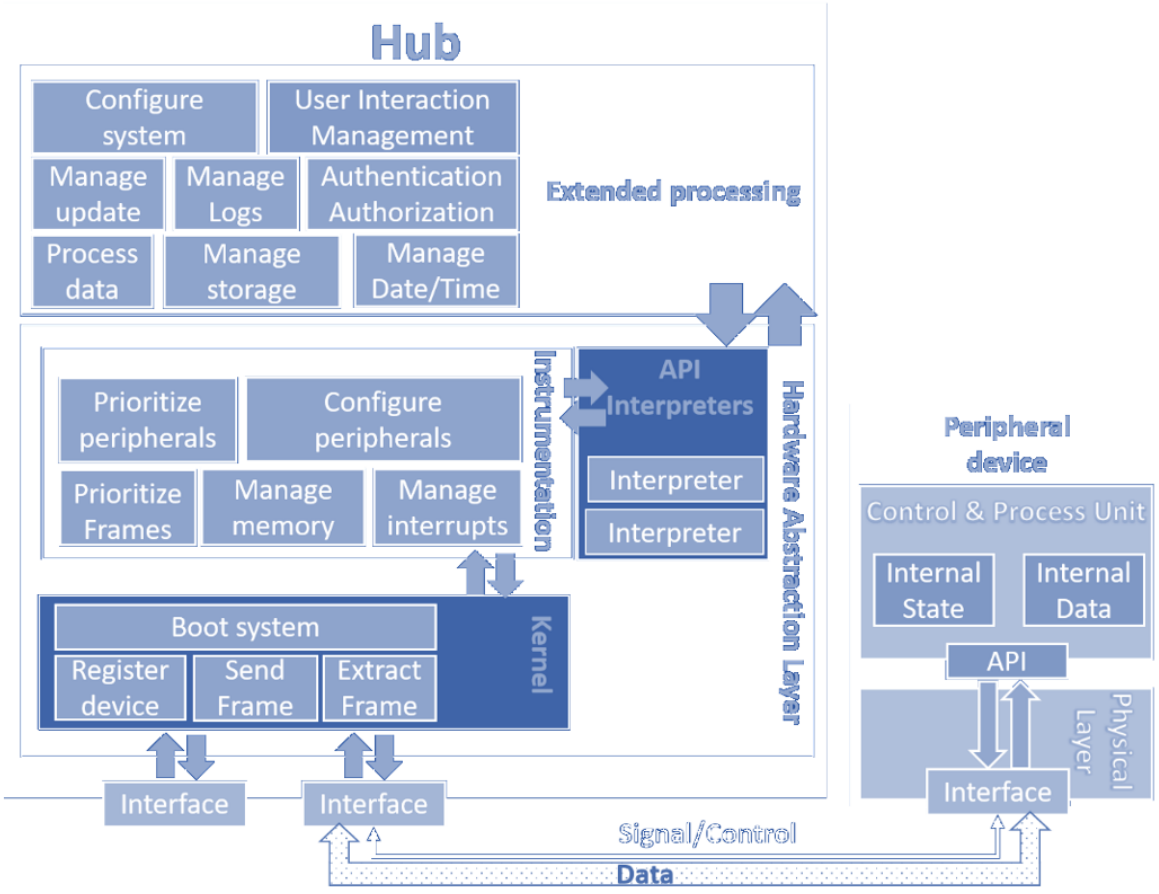

Figure 2.6 Central hub software architecture. Figure shows the relation and communication between peripheral device and SyncBox software.

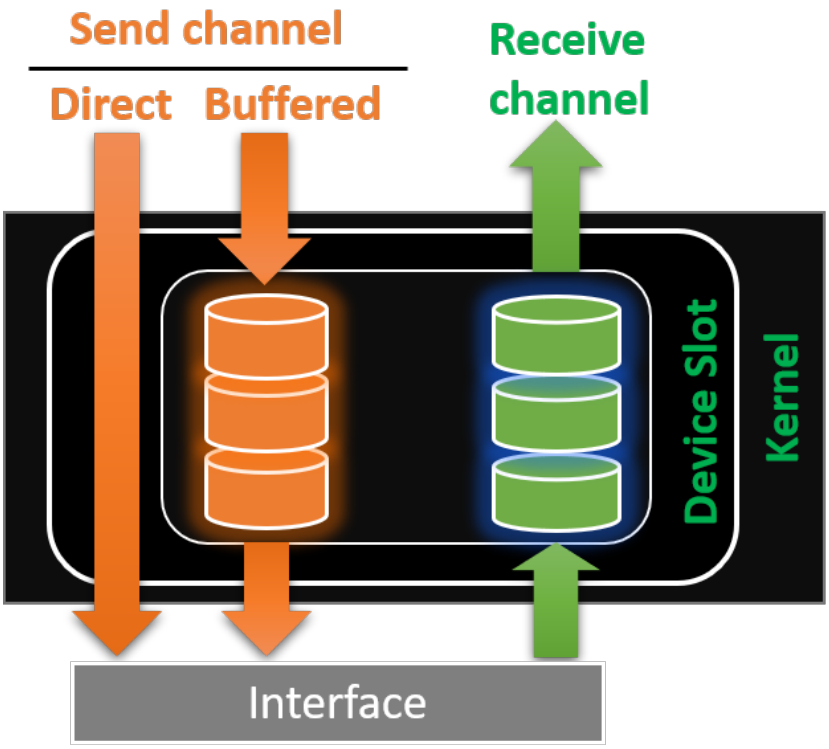

Figure 2.7 Figure shows a sample device slot structure within the kernel. Each device is a connected to a virtual bus within the kernel. Each slot provides one buffered send channel, one buffered receive channel and one direct pipeline.

The kernel assigns a specific memory location to each device. These locations are named as logical device slots and hard-coded within the kernel settings Each slot consists of two buffered channels, one for the sent data and the other for the received data, accompanied with a direct channel for non-buffered sent data that is useful for emergency cases. Again, following the same analogy, one could imagine that the secretary assigns three folders for each send-source, one for incoming messages from the sender, the other outgoing messages and the last folder is reserved for top priority messages, which are not actually buffered but directly passed for processing. During the boot process, kernel accomplishes the necessary controls and registers the peripheral devices into their appropriate slots.

Each massage stored within the send or receive channel of a slot has a specific format. It consists of a payload header and a delimiter trailer. Delimiter identifies the end of a frame and is usually specified within the peripheral device API-contract. By default, the kernel assumes that the messages are C-Style character strings terminated

at a '\0', but this assumption is not restricted and it is possible to change the delimiter of each device within the kernel configurations. In order to protect against memory overflow problem, the maximum frame size is set to be constant and determined by MAX_MSG_SIZE kernel parameter.

Kernel services (Figure 2.7) are used by the instrumentation section of HAL. These services relieve the instrumentation from getting involved into communication details (e.g. speed, protocol, control mechanisms, etc.) and allows it to directly receive messages in predetermined and organized frames.

The instrumentation section is called by the kernel after a successful boot-up. The kernel orchestrates the system workflow , interprets the incoming interrupts and triggers the peripherals with the most updated situations. The peripheral devices do not carry the same weight of importance. Some devices are required to respond within a specific time interval, otherwise malfunctions could occur. Most common malfunction scenarios are asynchronous work between X-ray and detector which results with insufficient or empty imaging result, delay or failure on the collision sensors. As a more serious example, if actuators do not receive a stop command in a timely manner, the patient may be harmed. In addition, messages of the same device type may have different levels of priorities. The instrumentation design is responsible for both types of prioritizations (i.e. prioritizing devices and messages). Instrumentation system is the core control section of the system. SyncBox device works with several peripheral devices by using their application programming interface (API). SyncBox main task is to monitor the actions coming from API's, prioritize them and send them to necessary peripheral devices in order. Instrumentation section requires to interact with peripheral APIs. Each manufacturer provides its own set of API and there is no common agreement on the details of the public functions signature. In order to alleviate this issue, the instrumentation employs interpreters. For each device type of each vendor, an interpreter is required for the instrumentation. Interpreters translate the messages coming from the peripheral API into a standard language that the instrumentation could understand. In the ideal case, whenever a peripheral device is replaced, it should be enough to add the appropriate interpreter to the interpretation

section. In addition, a device manufacturer may revisit the instrumentation section for optimizing their own setup if the default workflow does not meet their requirements.

2.3.4 Extended processing

The Extended Processing section is a collection of bulky operations, such as handling user interface, protocol preparation (patient type, energy level, mechanics positioning parameters), image processing, data management and integration with Radiology Information System (RIS) and Picture Archiving and Communication System (PACS). These operations are totally realizable in a high-level software (such as C++ or C#) and to execute such a program, an operating system is required (e.g. Linux, Windows).

2.4 Results

First hardware implementation of the SyncBox is shown in Figure 2.8, where each labeled section (a-r) presented is described in detail at Table 2. Both hardware design and the developed firmware are freely available [73] and could be customized for similar devices.

The firmware was prepared with MicroC pro version 7. The floating-point numbers were based on IEEE 754 32-bit and all integer values were two bytes little endian. The micro controller is externally tuned with an 8-Mhz crystal that is internally raised up to 140 Mhz.

The proposed architecture was implemented and used for assembling a full body scanner (Figure 2.9). In this device, Teledyne Time Delay Integration (TDI) detector (located under the patient table, labelled as Figure 2.9- D), Gulmay High frequency generator (B), X-ray tube (A) and Delta B2 motor controllers (C) were used.

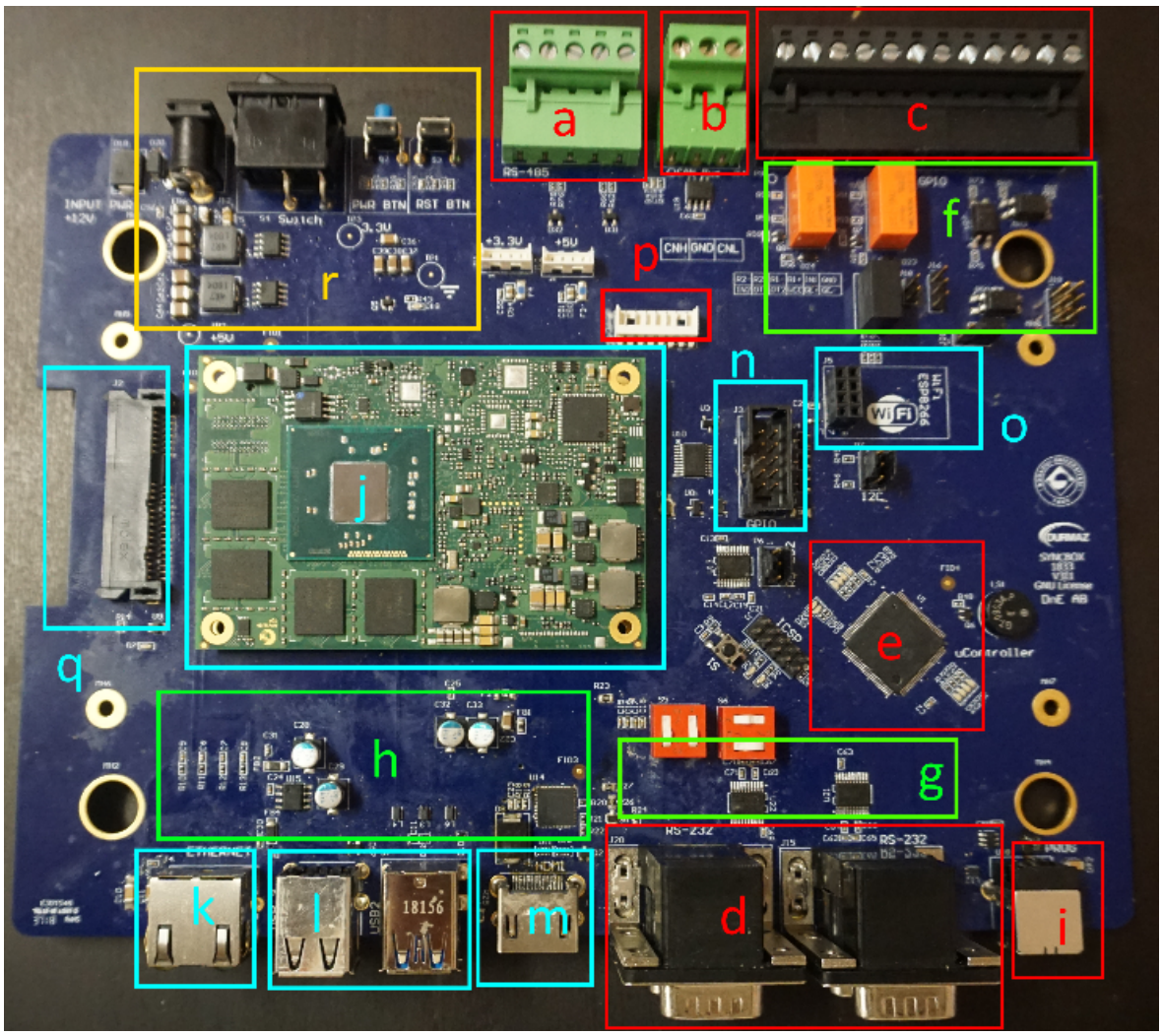

Figure 2.8 Implemented SyncBox device. The details of each unit are listed in Table 2. X-ray systems could use a variety of communication protocols. SyncBox has all the generic communication ports ready for future applications.

Table 2.3
Comparison between 3 whole body X-RAY scanner according to literature findings. Resolution and pixel pitch information is now available for EOS system.

	LODOX	EOS	X-LAB TDI BASED SCANNER
Scanning Time (seconds)	13	20	18
Radiation Dose (mGy)	0,33	0,92	0,76
Pixel Pitch (μm)	60	N/A	27
Image Resolution (lp / mm)	5	N/A	9
Main Focus	Trauma / Fractures	Scoliosis	Trauma / Emergency
Approximate Price	$335.000		$200.000

The developed system was designed with moving detector-source and static-object during X-ray exposure. TDI detector technology has a very high scanning resolution, but they are very sensitive to mechanical vibrations. In our device, the detector could scan 166 lines per cm and each line has approximately 27 µm resolution. To satisfy these requirements, the robotic unit was required to provide precise movement and stop mechanisms on a very short vibration amplitude. The robotic system could offer 20 µm step accuracy, up to 10 cm/sec movement speed. The details of the device connections are listed in Table 2.4.

A comparison has been made between commercial whole body imaging devices on the market. LODOX / Statscan is a digital x-ray scanner [74, 75]. It is mostly specialized in trauma patients, and fracture detection. EOS is a European based system, using a gaseous detector named MicroMegas [76] by G. Charpak et.al. TDI based whole body scanner developed in X-Lab, Boğaziçi University for to provide the proof of concept about our controller platform SyncBox. Conventional stitching method, Lodox, EOS, our new design. Table 2.4 is a basic comparison between 3 systems based on literature and technical findings.

The device was tested for both communication diversity and image consistency

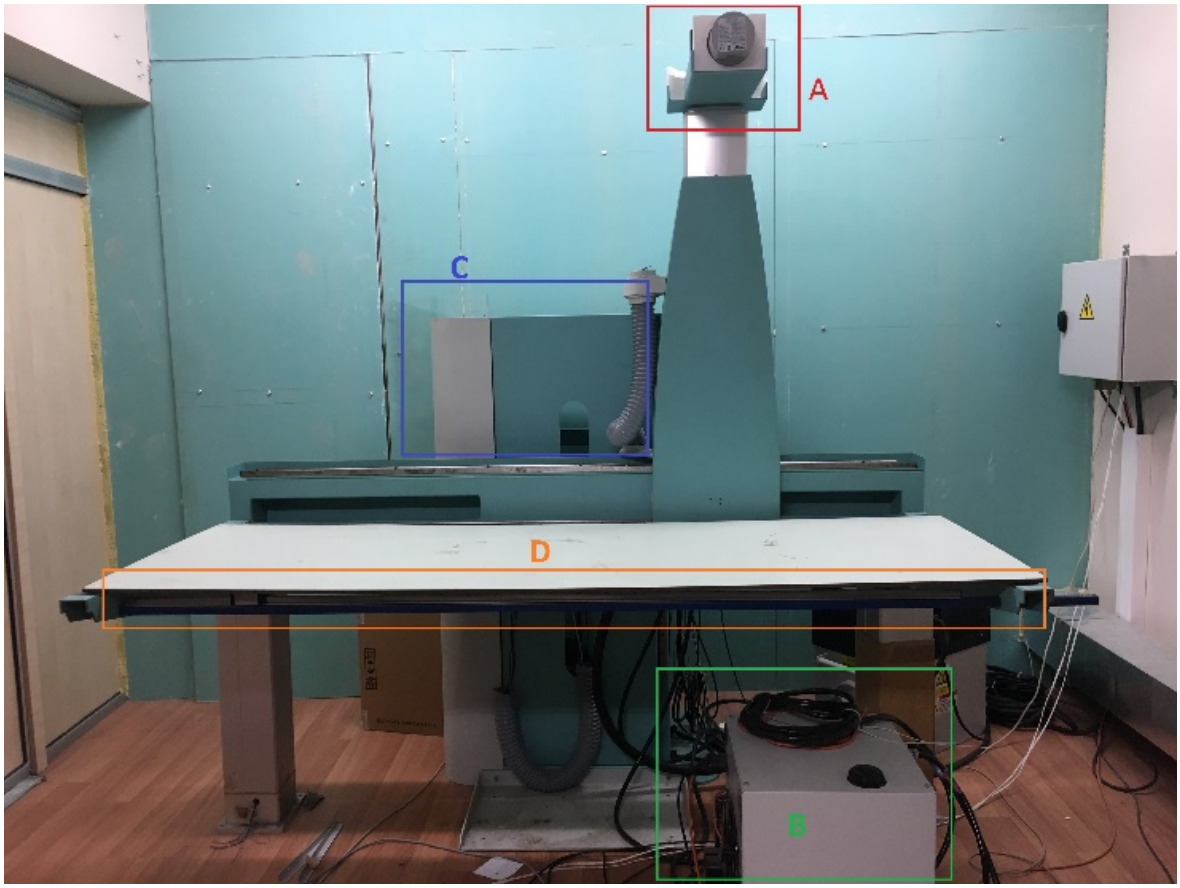

Figure 2.9 A TDI line scanner based full body X-ray scanner. SyncBox was employed to design and operate this configuration. A) X-ray tube B) High frequency generator system, C) Main body with servo motors, controllers and electrical system, D) Patient table combined with detector system. X-ray system includes all the main and some additional component that would be present in a standart X-ray system. For minimizing shifting between source, and detector, X-ray tube and line detector are moving along the same mechanical unit controlled by a single motor.

Table 2.4
Full X-ray Scanner Connections. This table shows an example X-ray system main component communication protocols. These protocols are the common standarts for X-ray devices.

Device	Type	Protocol	Connection
TDI - Teledyne Argus	Detector	Ethernet	GigE-RJ45
Servo Motor Driver - Delta B2	Actuator and Robotics	Modbus RTU	RS-232-DSUB9
Power Generator - Gulmay JA3200	Power Source	UART	RS-232-DSUB9

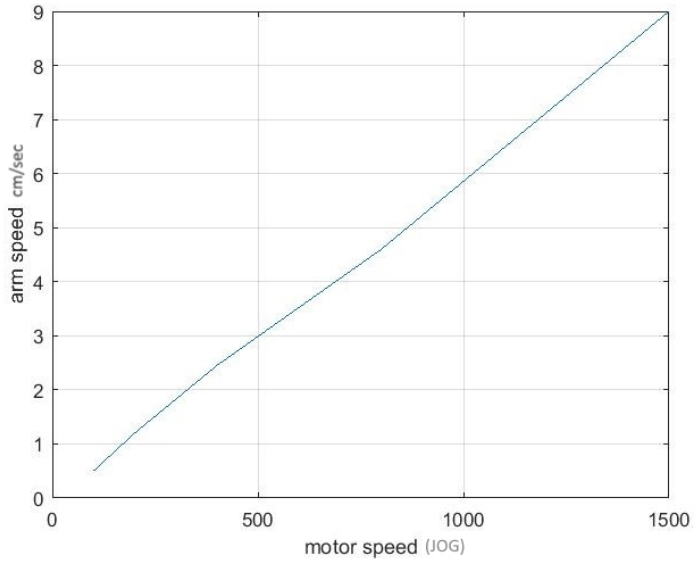

Figure 2.10 Motor speed connection chart. Experimental results of SyncBox communication with servo motor drives. The graph indicates the linearity between speed and control JOG parameter input. It is used to observe the stability of mechatronic system control of the SyncBox system.

in order to show that data flow was provided without loss and error.

2.4.1 Servo Driver Test

The servo driver was tested for measuring the smoothness of the arm movement. A range of motor rotation speeds was sent to the Delta-B2 servo controllers and the actuators move was measured (Figure 2.10). The output clearly depicted a smooth and linear relationship between the requested speed and the output displacement.

2.4.2 SyncBox Adaptability - Detector Switching

SyncBox unit was tested with two different sensors in order to prove that it is adaptable to be used with different components on an X-ray device. For this purpose, we changed the current TDI detector with a Toshiba FDX4343R CMOS Flat panel detector. We used Pro-Digi Pro-Project -02 -102, a CE certified phantom, which complies with IEC 61223-3-1 and DIN 6868/58 standards. Figure 11 shows X-ray images taken with two different detectors using the same generator and X-ray tube

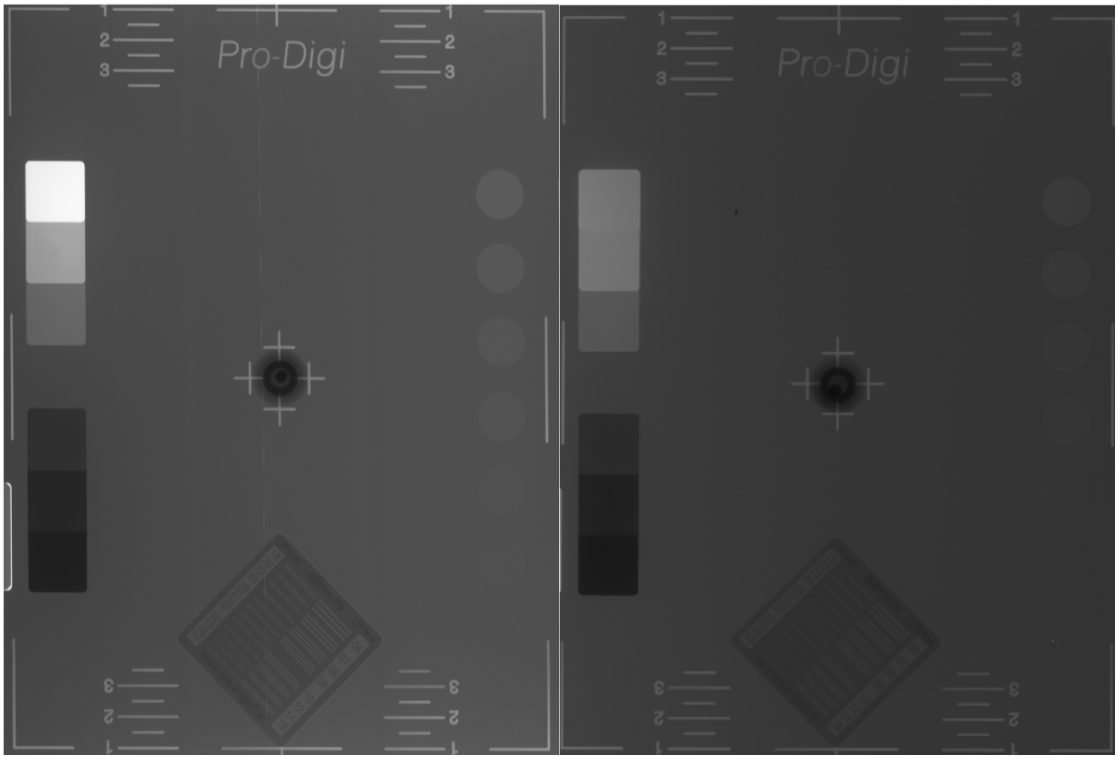

Figure 2.11 Pro-Digi Pro-Project -02 -102 phantom images for (left) a TDI detector and (right) a flat panel detector. Phantom images has been taken with same X-ray tube and generator. A standart bucky and alumunim grid has been used for flat panel detector. Results shows that TDI scanner has higher performance on contrast and resolution comparing to flat panel.

system along with the SyncBox interface. During this process, one detector was taken out of the system, while the new detector was installed with its own bucky unit. We have used the same generator and X-ray tube for testing. We have widen the collimator setting for the flat panel to able to get full imaging of the phantom. Mechanic movement system was disabled during flat panel image acquisition. The performance of images compared by using imageJ histogram tool. Each layer of step wedge phantom inside Pro-Digi Pro-Project -02 -102 has been checked for histogram. Mean contrast values and standard deviation values are recorded for homogeneity and contrast resolution [20]. According to results in Table 4 TDI detector offers higher contrast.

2.5 Discussion

The advancement in interoperable devices for medical applications is relatively new all through for the last 15 years. Academicians and regulatory bodies are actively

Figure 2.12 Victoreen Nuclear Associate Hand Phantom 76-634 x-ray image taken by SyncBox controlled TDI detector x-ray scanner. 0.5 mm aluminum filtration has been used. Exposure parameters are 60 kVp, 10 mA duration 1.8 sec. Total image acquisition time 5 seconds.

Table 2.5
Detector contrast comparison by using step wedge phantom inside Pro-Digi Pro-Project -02 -102. Each step histogram has been calculated using imageJ. Comparison variables are mean contrast value and standart deviation.

Step Value	TDI Detector		Flat Panel Detector	
	Standard Deviation	Mean Contrast Value	Standart Deviation	Mean Contrast Value
0	3.196	247	3.191	116
1	4.746	155	1.1744	108
2	2.148	103	1.180	85
3	1.147	69	1.125	62
4	0.694	47	0.977	43
5	0.633	37	0.809	32
6	0.710	32	0.982	26

working to find applicable solutions for these demands[77, 78, 79]. Open source platforms that supply physical infrastructure for data and signal transfer between medical systems are emerging; these allow devices and applications to be connected or disconnected on demand [80]. The standards, developed by regulatory bodies, sketch a generic system model for device interoperation, the equipment safety, security and usability characteristics. However, absence of a serious open source effort could meet these criteria impede the progress of the available platforms [69, 81].

Succesful integrability in medical devices could provide with open source and Plug-and-Play (PnP) streamlines to meet researchers' extensibility demands. Open source movement provided stable, elegant and cheap alternatives in daily life applications [82] and the PnP paradigm has a potential to ease device interoperability and human-machine interactions. There are several examples of medical open source hardware solutions in literature such as electrocardiogram, myoelectric prostheses, infusion pumps, physiological monitoring, EEG systems and even a CT Scanner [83, 80]. However, due to the tight regulations of medical device ecosystem, the users does not prefer to use open source solutions and PnP systems in order to comply with interoperable medical device standards [61, 65]. Recently, there have been some attempts [65] to change this mindset and bring the medical device industry closer to the PnP paradigm and make this industry more attractive for the open source community.

In practice, Medical PnP has already successfully been applied for sharing electronic health information [71]. A group at the University of Florida prototyped a system to synchronize X-ray radiography device with the patient's breathing cycle to improve the quality of the radiography on a ventilated patient [58]. There are other examples, where medical device interoperability and medical system integration improved patient safety especially on clinical engineering area such as prioritizing ventilation system alarms[55, 65]. Unfortunately, due to the inability to cross the "interoperability chasm", the slow pace medical device and health information technology (HIT) ecosystem is deprived from many other good ideas for improving patient care [84, 55].

In this paper, a new open source platform for developing interoperable radiogra-

phy devices is introduced, a version of this platform is implemented as SyncBox and is applied for developing a full body X-ray radiography device. Despite the available alternatives, the SyncBox targets to reuse existing components and infastructure to extend the creativity with modular blocks for developing safe and interoperable radiography systems. The actuator relocation smoothness and image quality were evaluated and the results showed that both criteria were satisfied within acceptable intervals. Additionally, a TDI detector was replaced by a Flat panel technology detector and SyncBox successfully integrated the detector with minimum efforts.

This platform aims to accelerate the realization of innovative novel designs with potential gain in development costs and time. This work is timely, since there is a trend within the radiography systems, shifting from "as-is" to "plug-integrate-play (PIP)" as the hardware design principle.

In contrast to the other open source interoperability platforms [80, 85, 86], which aim toward making connection in between end systems, the SyncBox brings the concept of the interoperability to the device design phase. The manufacturers and developers could build up a system specifically to meet their expectations using SyncBox. Health institutes, academic researchers and regulatory bodies could assemble their own customized radiography scanners based on their own necessities. This platform democratizes the X-ray device manufacturing process and breaks the prefabricated device design limitations (such as detector and power source choices) on acquired data. In long term, this platform could lead the way for more cost-effective radiography devices and reduce the device manufacturing time.

SyncBox has a potential to extend its usage area to many platforms, starting with fluoroscopy and mammography devices due to working principle to direct x-ray systems. In theory it could be extended in the future to support other modalities, such as ultrasound devices or multimodality imaging systems. It has a potential to communicate and control many different devices which could be extended to several other hardware-like transducers, or advanced mechanics. However, these implementations need a collaborative effort and significant support from different imaging device

Table 2.6
SyncBox based - OEM device comparison. SyncBox based device could be upgrade, customized or convert to a different modality such as from DR to a mammography device components could be replaced easily. On the other hand, three could be problems on the stability, and certification process such as CE or FDA should be completed by the end user.

Section	SyncBox based X-Ray System	OEM X-Ray DR Systems
Integrability	Full	Partial
Extensibility	Full	None
Upgradability	Full	Partial
Customizability	Full	Partial
Standard Compatibility	Partial	Partial
Inter-operability	Full	Partial
Stability	Relative	Stable
Cost	$50.000 - $400.000	$80.000 - $300.000

component vendors and research teams, for the required API integrations and software development. Performance comparison between SyncBox and conventional OEM system development has been made using several factors (Table 2.6). SyncBox offers flexible solutions for end users, on the other commercial products may offer more stable products. SyncBox offered as an open source platform for users, however device cost is depending on several variables such as component prices and integration cost. SyncBox has several advantages over the OEM and pre designed systems on integrability, extensibility, upgradability, customizability.

2.6 Conclusion

The SyncBox model and its implementation followed the best practices of software and electrical engineering. All aspects of the system were modeled and documented in different levels of technical details. These models and documentations are shared across communities of researchers and manufacturers to enable them to leverage and reuse, with their own software and hardware components. We believe that the "SyncBox approach" has a great potential for cost effective, standardized, and faster prototype production for innovative medical imaging devices. Once the SyncBox is applied by different research groups and improved further within its open platform

format by all, it could have a chance in becoming a standard R&D tool for innovative medical imaging products in the future.

3. FULL BODY X-RAY SCANNER

Whole body X-ray scanning is relatively new technology, however, it has found its way in medicine in different applications such as imaging for trauma and bone densitometry measurement [87, 88, 89, 90]. Improvement on digital imaging technologies reveals new opportunities for whole body system imaging, such as higher resolution, radiation dose management and 3D imaging [91, 92, 88]. TDI controlled whole body X-ray imaging system is designed to obtain very high-resolution images with continuous X-ray exposure a model can be seen on Figure 3.1. It has commonly used in security and non-destructive testing applications. [93, 94].

3.1 Full Body X-ray Devices

3.1.1 EOS

The EOS X-ray is the one of the first scanners in the world that creates full-body 3D images of patients in standing position as shown in Figure 3.1. It provides orthopedic imaging for patients with spine, hip, and leg disorders. Based on the manufacturer claims EOS works in much less radiation than traditional scanners [92, 91].

3.1.2 LODOX Statscan

Lodox Statscan is produce a full body image body in 13 seconds using linear slit scanning radiography (LSSR) [88]. The device is designed for different applications such as ventriculoperitoneal (VP) shunt visualization, emergency room arteriography (ERA), detection of foreign bodies, and pediatric emergency imaging are presented [95, 13, 75, 74]. A trauma patient over LODOX Statscan device has shown in Figure 3.2.

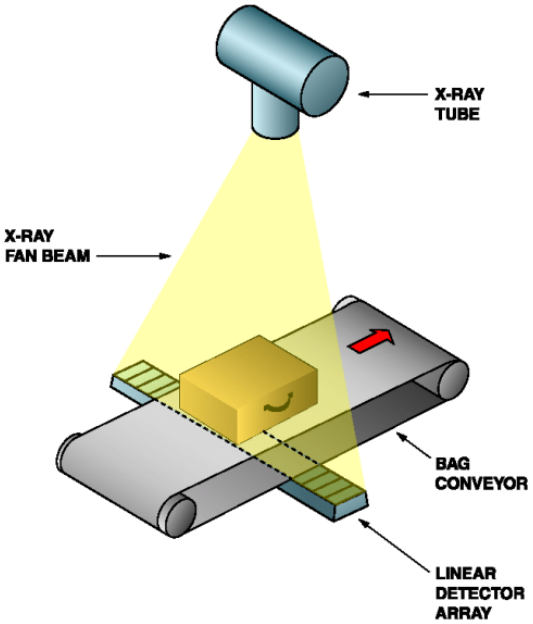

Figure 3.1 Luggage X-ray inspection system using linear detector array. It could able to investigate 1500 luggage / hour [11].

Figure 3.2 EOS system designed for 2D and 3D image acqusitions, system detector and X-ray source parts are vertically moving to get a biplaner digital images [12].

Figure 3.3 Lodox Statscan on a trauma patient. System is mounted on the wall, movement is on one direction [13].

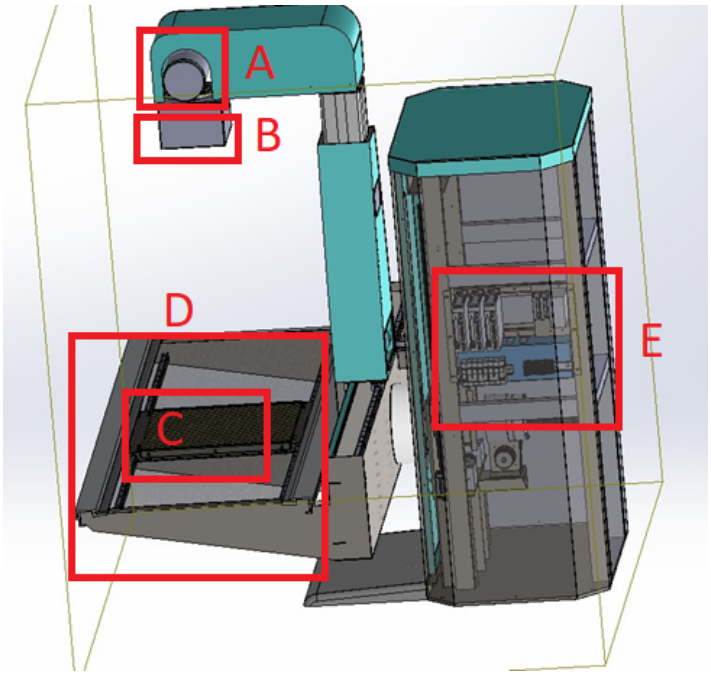

Figure 3.4 Main units connected to the system, also explained in the table 2.5. (A) X-Ray Tube, (B) Collimator, (C) X-Ray Detector, (D) Table, (E) Control and Driver.

3.2 X-ray System Design

Despite the similar functionalities, the mechanical and actuators of the new full body scanner is revisited to optimize the reusability, manufacturability and flexibility aims. The hard core of the design is a sliding C-Arm on top of fixed table. Figure 3.4. shows the component location with respect to each other and Table 3.1 describes each unit in more detail. Main aim of our research is to create a flexible device infastructure for general diagnostic purposes. Mechatronic system also has been designed and manufactured with the same vision.

Despite the EOS (moves in just top-to-bottom direction) and LODOX design (scans only horizontally), the designed mechanisms provide scanning in any direction. This facility is provided by means of two independent motors with different powers. To rotate the table in -90 to +90 degrees a strong 2.3kw delta ac servo motor has been used. This motor is connected to the table through precise reduction gearbox and a 70mm shaft to the table as in Figure 3.5

Table 3.1
Main Parts connected to X-ray mechanical system.

	Part	Description
A	X-ray Tube	The housing is designed for common cylindrical X-ray tubes. It supports up to 50 Kg.
B	Collimator	Slit and rectangular collimators are supported. The attachment of the detector to collimator is flexible. In some cases, a few junction units may require adapting the collimator to X-ray tube.
C	X-ray Detector	The detector is mounted on top of two precise anti friction linear guide slide rails. These rails provide a great performance on damping small vibrations. The housing provides even up to 50 cm detector length.
D	Table	The tabletop is medical radio lucent.
E	Control and Driver	A combination of a PLC and motor drivers are used to provide a flexible control over device moves.

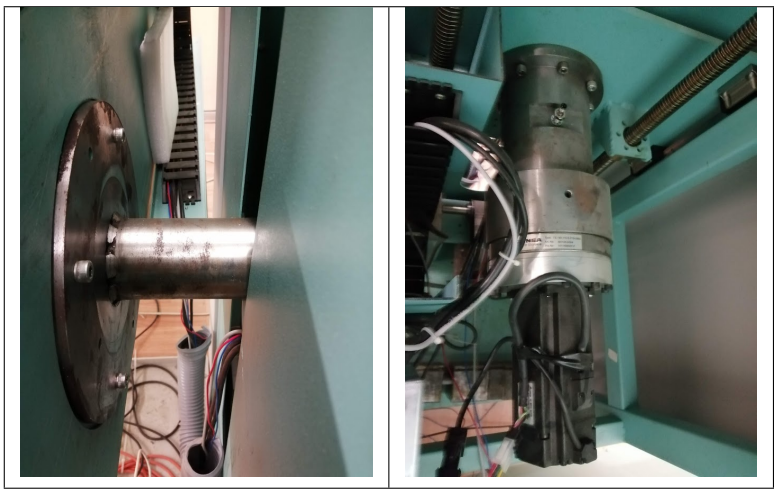

Figure 3.5 Table rotation shaft and AC motor for rotational movement.

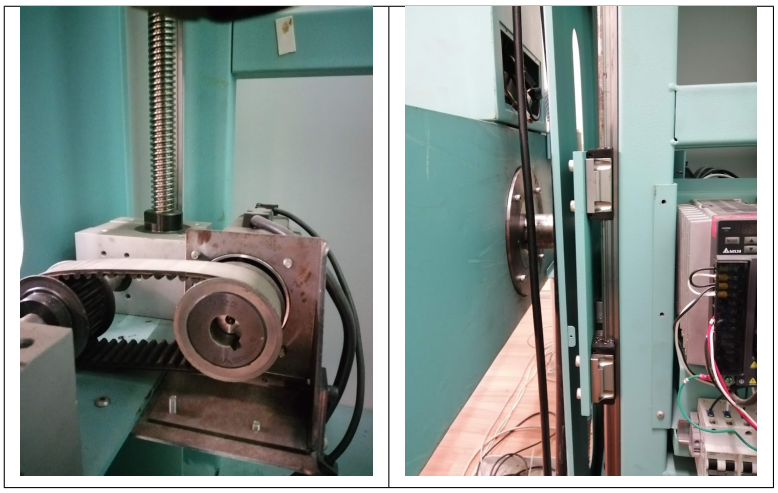

Figure 3.6 A worm drive is used to move the table top and bottom, B- sliding rails are used to absorb the vibrations.

In addition to table rotation, in our design it is possible to adjust table height. For this, worm drive is used (Figure 3.6- A). To reduce the vibration of the worm drive, another rail mechanism also added (Figure 3.6-B). Another servo motor provides the required power these mechanisms.

The sliding mechanism is powered via another motor. The rotation of the motor is converted to a linear motion through a gear rail as shown in Figure 3.7.

The other key advantage of our deign over the LODOX and EOS is flexible Source Image Distance (SID). Beneath the X-ray tube there is a telescopic column which provides an adjustable length. By tuning this length, it is possible to control the amount of energy received by the patient body as in Figure 3.8.

Altough it is a more complex design than the similar devices it should be considered that the design is flexible and provides accurate and precise motion. This motion could be extended to other applications more readily. For example, if required, one can use a resized version of this design to manufacture a TDI mammography or cephalography.

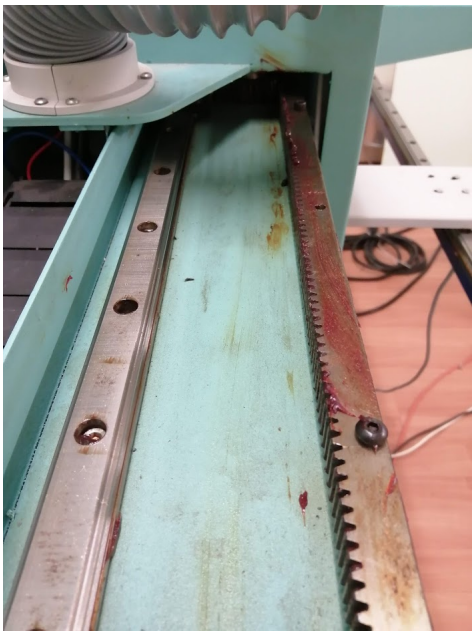

Figure 3.7 Gear rail provides sliding path for the C-Arm.

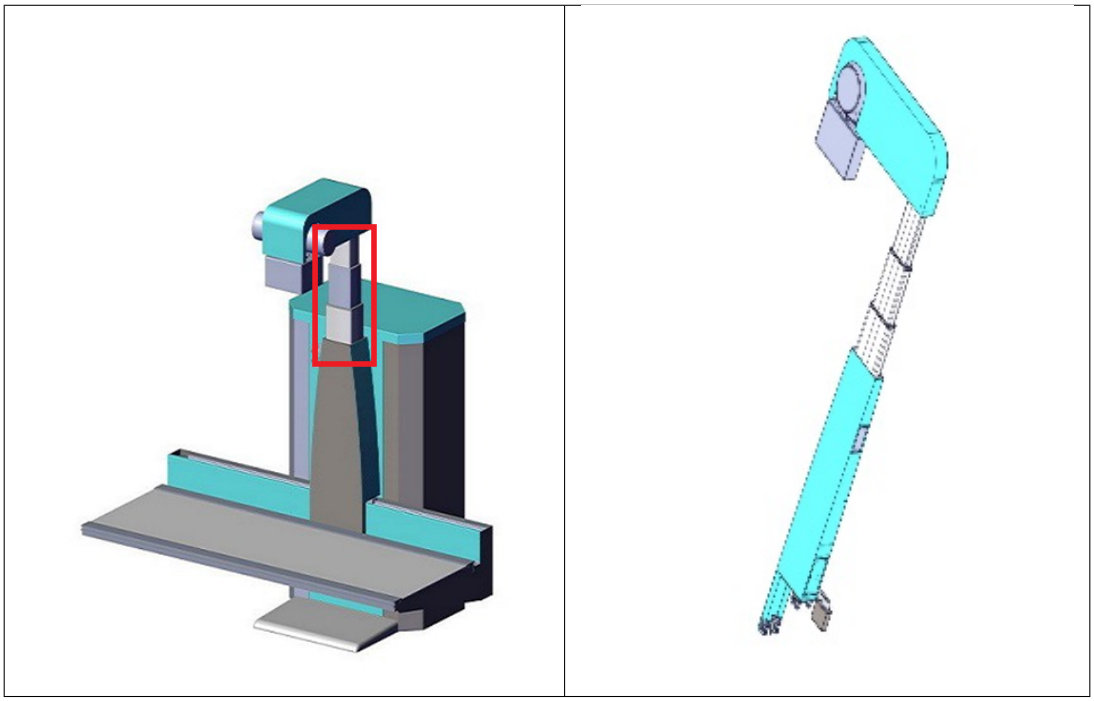

Figure 3.8 Telescopic column provides a flexible SID.

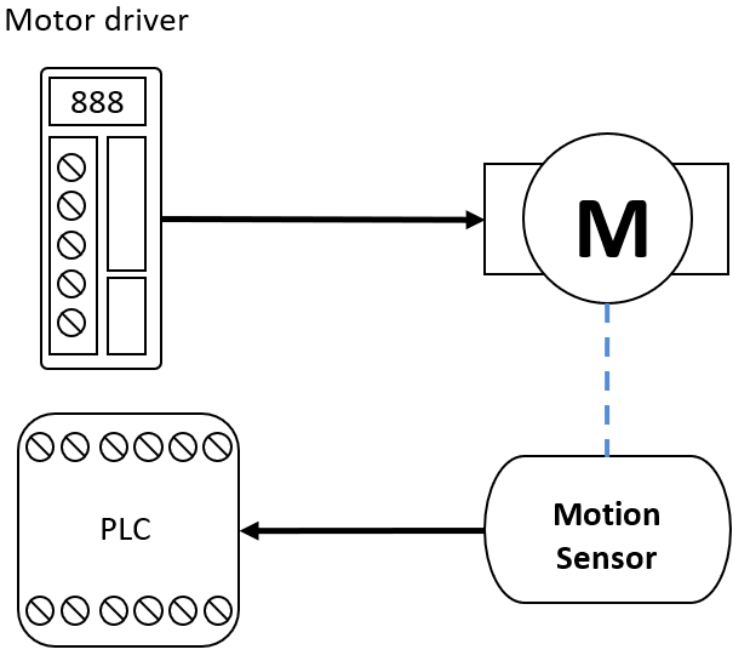

Figure 3.9 Schematic diagram of the motor control system.

3.3 Feedback System

A simplified feedback diagram of the system is shown in the Figure 3.9. In this diagram motor driver provides the power to motor in response to requested torque and speed. Motion sensors monitor the rotation and location of the actuators and provide the feedback to a PLC. This design provides digital control all on sensors, and motor systems from a simple interface.

The control system is shown in Figure 3.10. In this diagram each motor has its own unique servo driver, but all sensors data are collected in one PLC. To provide an extra protection safety fuses are also included.

The communication between motor drivers and the central workstation is accomplished through SyncBox [96]. This device provides a unified solution to all peripherals and device parameters. It controls the servomotors, read the sensor values, monitor air conditioning systems, and communicate with power generator. In this way all the monitoring and controlling tasks are done in one solution. A simple diagram that shows

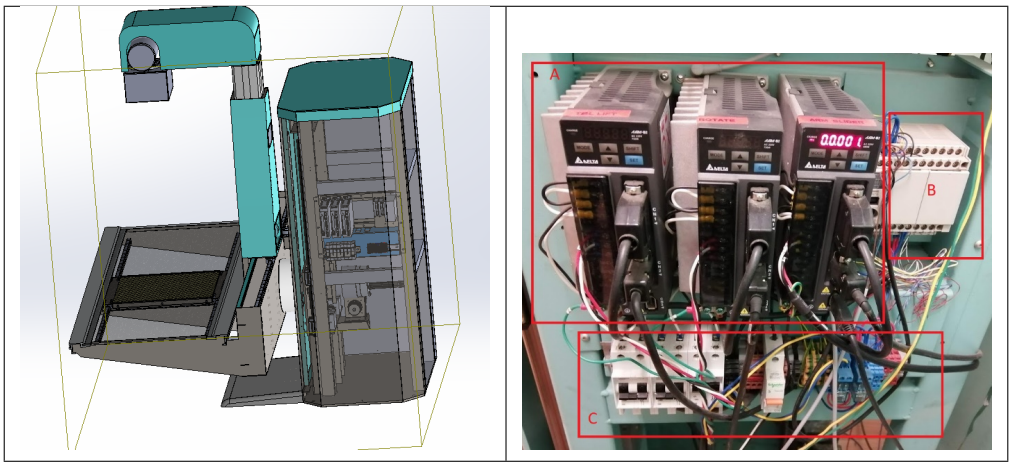

Figure 3.10 Left hand side: General placement of servo-motor systems, Right hand side: A) servo-motor drivers B) PLC C) power lines.

the peripherals are shown in Figure 3.11.

3.4 SyncBox Control

Syncbox System, and it's functions are explained in detail in Chapter 2.1. Syncbox has improved over time from a basic microcontroller unit to a combined system with an advance microcontroller and microprocessor unit as shown in Figure 3.12. System works combined with IBEX software module [14]. Interface of the IBEX module has been showed in Figure 3.13. Syncbox able to control all motor drivers, and sensors along with the high frequency generator, and TDI detector from a central control unit.

3.5 Results

The performance of the TDI detector strongly depends on the quality of the device actuators precision, vibration, and speed. It is well-known in mechanical systems that increasing the system speed could cause system overshoot [97] and as a result systems starts to vibrate, however reducing the system movement speed could solve this problem but on the other hand it would lead to patient overdose. As a result a precisely calibrated mechanical system is inevitable. In Figure 3.14 and 3.15 the

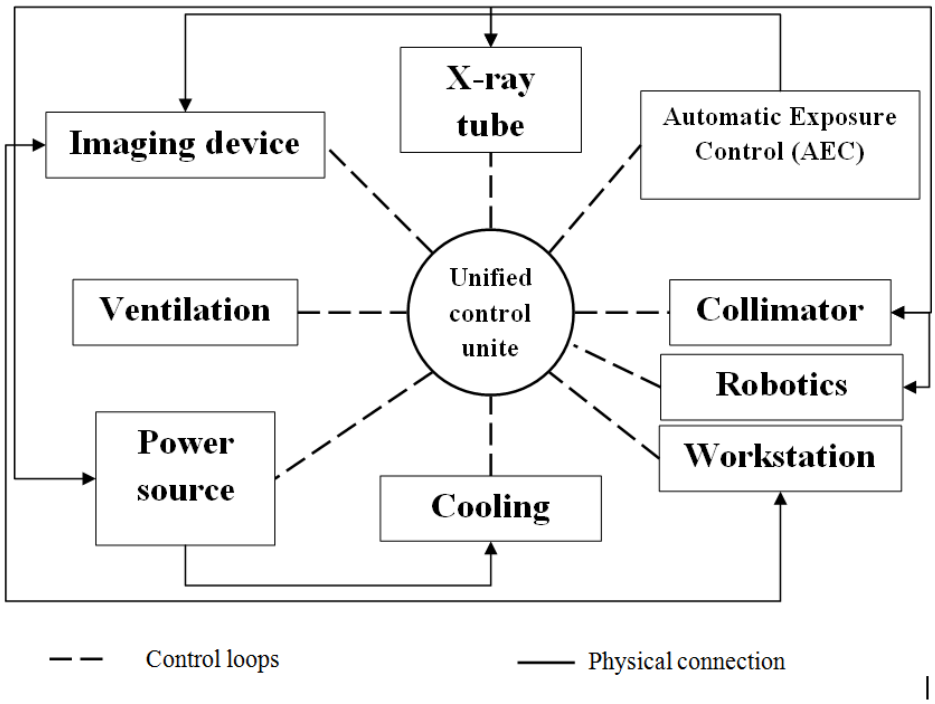

Figure 3.11 SyncBox provides a unified control solution for all device and peripheral parameters.

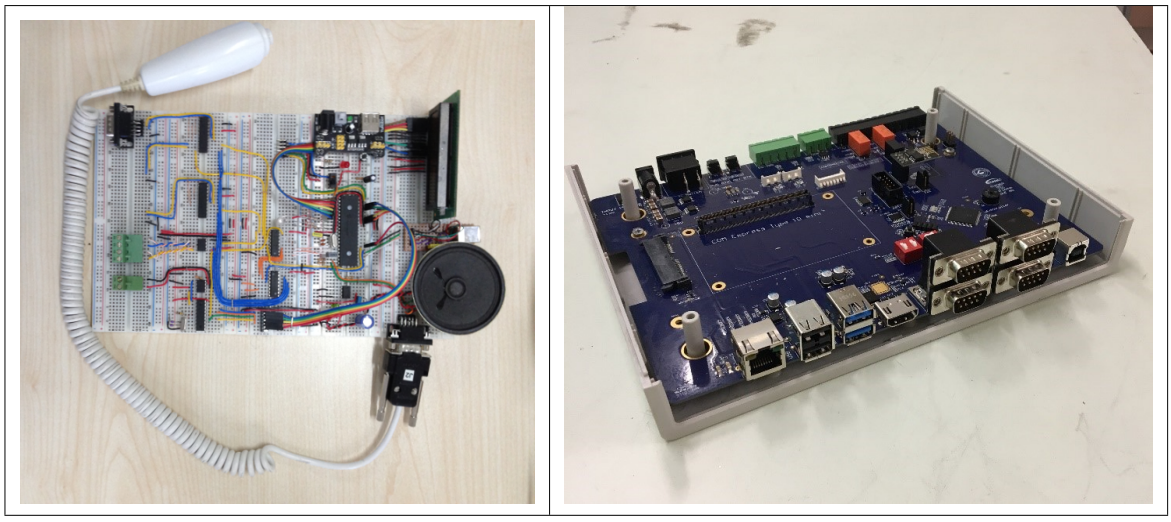

Figure 3.12 Syncbox v1.0 and v3.3. v1.0 designed with a 8 bit microcontroller to able to control the high frequency generator, and able to trigger flat panel detector (Toshiba FDX 4343R). Current version able to control more than 20 different units, acquire and process the images, connect to a network system and display and control the system with an internal microprocessor.

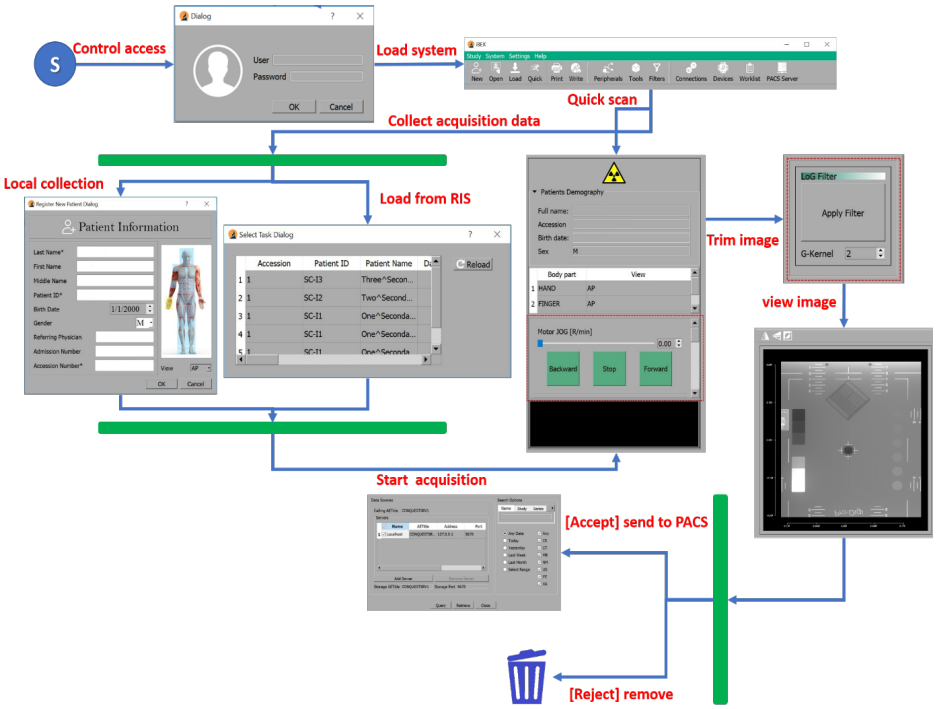

Figure 3.13 IBEX workflow and interface [14]

applied calibration parameters for the sliding motor is shown. Figure 3.16 and Figure 3.17 are the first succesful result taken from the designed device with a step phantom.

Additionally, calibration increases the motor performance and lifespan. Figure 2.26 shows the closed loop system performance on a wide range of input frequencies. As it is shown in this figure, the closed loop system bandwidth is up to 500HZ, which is far more than what is normally used in our design.

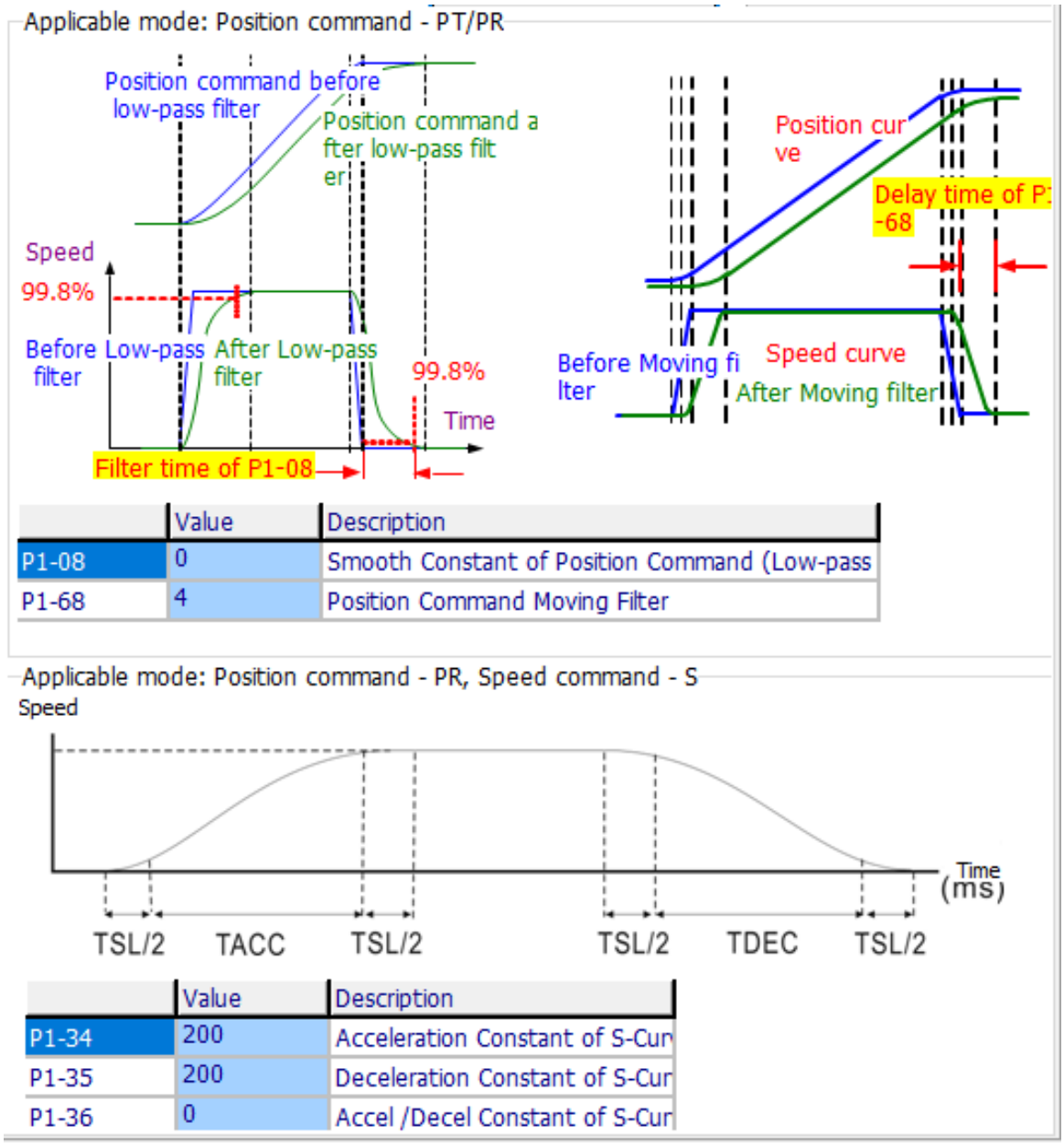

	Value	Description
P1-08	0	Smooth Constant of Position Command (Low-pass
P1-68	4	Position Command Moving Filter

	Value	Description
P1-34	200	Acceleration Constant of S-Cur
P1-35	200	Deceleration Constant of S-Cur
P1-36	0	Accel /Decel Constant of S-Cur

Figure 3.14 Calibration parameters of the servo motor for Position Control (PT) mode.

Figure 3.15 Motor behaviour under different frequencies. Top figure is magnitude bottom phase diagram. System is calibrated with low frequencies combined with TDI parameters.

Figure 3.16 Contrast phantom image output after the calibration of TDI detector frequency, motor system calibration, and X-ray parameters optimization.

Figure 3.17 Anotomical Image Result from X-Lab X-Ray Scanner.

4. CONCLUSION AND FUTURE WORKS

Digital radiography devices are widely used every day. As an outcome of this study a whole-body X-ray scanner system is assembled and controlled througha novel control hardware device, not available in the current state-of-the-art commercial or experimental systems. This control hardware, SyncBox, is able to acquire signals from moving gantry system, and combine the data. During imaging sequence SyncBox will be able to monitor, and control all parts of the system. Mechanical, mechatronics, electronics, electrical aspects of the whole body X-ray system has been designed and integrated around this novel SyncBox during this dissertations work. All system has been calibrated and documented. Research about the Syncbox system has been published, and the source code of the design has been shared open source [73].

4.1 Open Source Medical Device Enviorement

During the time of this dissertation work designing a new type of X-ray device has evolved to have a wider potential. It has been presented here that creating an open source enviroment for medical devices is possible with today's modern technologies. We are able to demonstrate a proof of concept towards this overall ideal, and develop its first core component, a plug-integrate device to control and monitor a full body X-ray scanner. The open platform model and its first implementation has been succesfuly established. All the aspects of the system were modeled and documented in different levels of technical details. These models and documentations are shared across communities of researchers and manufacturers to enable them to leverage and reuse, with their own software and hardware components. We believe that the "Open platform medical device model" has a great potential for faster, better and cheaper prototype production for innovative medical imaging devices. Once the platform is applied by different research groups and improved further within its open platform format by all, it could have a chance in becoming a standard R&D tool for innovative medical imaging products in the future.

4.2 Future Works

There are several open problems, and significant amount of additional effort is needed to complete these:

- **Open source medical parts**: Designing new parts for medical imaging is an essential part of the process. One of the difficulties we have met over time is the limited SDK's and completely closed circuit systems. Development of the new flexible hardware will be a faster way for to develop more and better devices over time.
- **Improve the documentation and qualification on platform:** Altough we provided main documentation for the SyncBox development platform, and give away source codes, more detailed documentation is needed both on development and user side of the system.
- **Testing the platform with other medical diagnostic devices:** As a scope of this thesis we have been establised a new generation direct X-ray device and combine it with our platform. Using a similar platform on different medical devices such as fluoroscopy, mammography will improve the hypothesis, and develop an open source community on medical diagnostic.
- **Clinical testing and certification process:** Testing the device on clinical enviroment, and clinical research will be a milestone for open source medical diagnostic. System will be validated and will be accessible for clinical usage.
- **Advanced image processing modules for specific applications and, cloud platform integration:** As a part of todays industry principle, cloud sharing platforms, and advance software tools will improve the system. 3D imaging, multi energy studies, computed aided diagnosis tools will improve the structure of the platform, and supports the device especially on clinical levels.
- **Research and Development on non-medical platforms:** Syncbox also could be an alternative platform for developing devices on industrial, and security applications.

Each of these headings above could create new research long term research tracts, and hopefully new students and researchers pick up this dream and continue to lay the foundation towards the long road ahead for the democratization of medical imaging hardware.

REFERENCES

1. Feyzi, E., *Rontgen Su'A'ATI ve Tatbikat-i Tibbiye ve Cerrahiyesi*, 1898.

2. Beutel, J., H. L. Kundel, and R. L. Van Metter, *Handbook of Medical Imaging*, Vol. 1, Spie Press, 2000.

3. Sobol, W. T., "High frequency x-ray generator basics," *Medical Physics*, Vol. 29, no. 2, pp. 132–144, 2002.

4. Roque, R. J. d. C., "X-ray imaging using 100 μm thick gas electron multipliers operating in kr-co2 mixtures," Master's thesis, 2018.

5. Yaffe, M., and J. Rowlands, "X-ray detectors for digital radiography," *Physics in Medicine & Biology*, Vol. 42, no. 1, p. 1, 1997.

6. Allisy-Roberts, P. J., and J. Williams, *Farr's Physics for Medical Imaging*, Elsevier Health Sciences, 2007.

7. Walter, D., U. Zscherpel, and U. Ewert, *Photon Counting and Energy Discriminating X-Ray Detectors-Benefits and Applications*, Bundesanstalt für Materialforschung undprüfung (BAM), 2016.

8. Tousignant, O., M. Choquette, Y. Demers, L. Laperriere, J. Leboeuf, M. Honda, M. Nishiki, A. Takahashi, and A. Tsukamoto, "Progress report on the performance of real-time selenium flat-panel detectors for direct x-ray imaging," in *Medical Imaging 2002: Physics of Medical Imaging*, Vol. 4682, pp. 503–510, International Society for Optics and Photonics, 2002.

9. Bulayev, Y., "Tdi imaging: An efficient aoi and axi tool,"

10. X-Scan Imaging Corp, *XTI-Harrier-CCD X-Ray Time Integration (TDI) CCD Camera*, 2018. Rev. 20190408.

11. Zentai, G., "X-ray imaging for homeland security," *International Journal of Signal and Imaging Systems Engineering*, Vol. 3, no. 1, pp. 13–20, 2010.

12. Illés, T., and S. Somoskeöy, "The eosâ¢ imaging system and its uses in daily orthopaedic practice," *International Orthopaedics*, Vol. 36, no. 7, pp. 1325–1331, 2012.

13. Mulligan, M. E., and C. W. Flye, "Initial experience with lodox statscan imaging system for detecting injuries of the pelvis and appendicular skeleton," *Emergency Radiology*, Vol. 13, no. 3, pp. 129–133, 2006.

14. Brusan, A., F. A. Durmaz, A. Yaman, and C. Öztürk, "ibex: Modular open-source software for digital radiography," *Journal of Digital Imaging*, pp. 1–14, 2019.

15. Ergüder, İ. B., F. A. Durmaz, A. Yaman, and C. Öztürk, "Design of a control circuit for x-ray generator," in *2016 20th National Biomedical Engineering Meeting (BIYOMUT)*, pp. 1–3, IEEE, 2016.

16. Gezer, M. C., O. Algin, A. Durmaz, and H. Arslan, "Efficiency and reporting confidence analysis of sequential dual-energy subtraction for thoracic x-ray examinations," *Qatar Medical Journal*, Vol. 2019, no. 1, p. 9, 2019.

17. Prince, J. L., and J. M. Links, *Medical imaging signals and systems*, Pearson Prentice Hall Upper Saddle River, NJ, 2006.

18. Glasser, O., "Wc roentgen and the discovery of the roentgen rays.," *AJR. American Journal of Roentgenology*, Vol. 165, no. 5, pp. 1033–1040, 1995.

19. Johns, H. E., and J. R. Cunningham, "The physics of radiology," 1983.

20. Wolbarst, A. B., and G. Cook, "Physics of radiology," 1993.

21. Klassen, S., "The photoelectric effect: Reconstructing the story for the physics classroom," 2011.

22. Eisenberger, P., and P. Platzman, "Compton scattering of x rays from bound electrons," *Physical Review A*, Vol. 2, no. 2, p. 415, 1970.

23. Fernandez, J., "Rayleigh and compton scattering contributions to x-ray fluorescence intensity," *X-Ray Spectrometry*, Vol. 21, no. 2, pp. 57–68, 1992.

24. Samei, E., M. J. Flynn, H. G. Chotas, and J. T. Dobbins III, "Dqe of direct and indirect digital radiography systems," in *Medical Imaging 2001: Physics of Medical Imaging*, Vol. 4320, pp. 189–197, International Society for Optics and Photonics, 2001.

25. Samei, E., and M. J. Flynn, "An experimental comparison of detector performance for direct and indirect digital radiography systems," *Medical Physics*, Vol. 30, no. 4, pp. 608–622, 2003.

26. Clark, G. L., *Applied X-rays*, McGraw-Hill Book, 1955.

27. Webb, S., "The physics of medical imaging-medical science series," 1996.

28. Boone, J. M., and J. A. Seibert, "An accurate method for computer-generating tungsten anode x-ray spectra from 30 to 140 kv," *Medical Physics*, Vol. 24, no. 11, pp. 1661–1670, 1997.

29. Tucker, D. M., G. T. Barnes, and X. Wu, "Molybdenum target x-ray spectra: A semiempirical model," *Medical Physics*, Vol. 18, no. 3, pp. 402–407, 1991.

30. Marshall, M., L. Peaple, G. Ardran, and H. Crooks, "A comparison of x-ray spectra and outputs from molybdenum and tungsten targets," *The British Journal Of Radiology*, Vol. 48, no. 565, pp. 31–39, 1975.

31. Boone, J. M., T. R. Fewell, and R. J. Jennings, "Molybdenum, rhodium, and tungsten anode spectral models using interpolating polynomials with application to mammography," *Medical Physics*, Vol. 24, no. 12, pp. 1863–1874, 1997.

32. Lehmann, L., R. Alvarez, A. Macovski, W. Brody, N. Pelc, S. J. Riederer, and A. Hall, "Generalized image combinations in dual kvp digital radiography," *Medical Physics*, Vol. 8, no. 5, pp. 659–667, 1981.

33. Parks, E. T., and G. F. Williamson, "Digital radiography: an overview," *J Contemp Dent Pract*, Vol. 3, no. 4, pp. 23–39, 2002.

34. Hoppe, R., T. L. Phillips, and M. Roach, *Leibel and Phillips Textbook of Radiation Oncology-E-Book: Expert Consult*, Elsevier Health Sciences, 2010.

35. Marchiori, D., *Clinical Imaging-E-Book: With Skeletal, Chest and Abdomen Pattern Differentials*, Elsevier Health Sciences, 2004.

36. Kotter, E., and M. Langer, "Digital radiography with large-area flat-panel detectors," *European Radiology*, Vol. 12, no. 10, pp. 2562–2570, 2002.

37. Lemoigne, Y., and A. Caner, *Molecular Imaging: Computer Reconstruction and Practice*, Springer Science & Business Media, 2008.

38. Korner, M., C. H. Weber, S. Wirth, K.-J. Pfeifer, M. F. Reiser, and M. Treitl, "Advances in digital radiography: physical principles and system overview," *Radiographics*, Vol. 27, no. 3, pp. 675–686, 2007.

39. Kim, H. K., G. Cho, S. W. Lee, Y. H. Shin, and H. S. Cho, "Development and evaluation of a digital radiographic system based on cmos image sensor," in *2000 IEEE Nuclear Science Symposium. Conference Record (Cat. No. 00CH37149)*, Vol. 3, pp. 23–33, IEEE, 2000.

40. Smith, S. T., D. R. Bednarek, D. C. Wobschall, M. Jeong, H. Kim, and S. Rudin, "Evaluation of a cmos image detector for low-cost and power medical x-ray imaging applications," in *Medical Imaging 1999: Physics of Medical Imaging*, Vol. 3659, pp. 952–961, International Society for Optics and Photonics, 1999.

41. Su, Y., W. Ma, and Y. M. Yang, "Perovskite semiconductors for direct x-ray detection and imaging," *Journal of Semiconductors*, Vol. 41, no. 5, p. 051204, 2020.

42. Del Sordo, S., L. Abbene, E. Caroli, A. M. Mancini, A. Zappettini, and P. Ubertini, "Progress in the development of cdte and cdznte semiconductor radiation detectors for astrophysical and medical applications," *Sensors*, Vol. 9, no. 5, pp. 3491–3526, 2009.

43. Kasap, S., J. B. Frey, G. Belev, O. Tousignant, H. Mani, J. Greenspan, L. Laperriere, O. Bubon, A. Reznik, G. DeCrescenzo, *et al.*, "Amorphous and polycrystalline photoconductors for direct conversion flat panel x-ray image sensors," *Sensors*, Vol. 11, no. 5, pp. 5112–5157, 2011.

44. de Groot, J., J. Holleman, H. Wallinga, M. Beerlage, H. Levels, and H. Mulder, "X-ray image sensor based on an optical tdi-ccd imager," in *Solid-State Imagers and Their Applications*, Vol. 591, pp. 24–30, International Society for Optics and Photonics, 1986.

45. Ercan, A., L. Haspeslagh, K. De Munck, K. Minoglou, A. Lauwers, and P. De Moor, "Prototype tdi sensors in embedded ccd in cmos technology," in *Int. Image Sensor Workshop*, 2013.

46. Baru, S., A. Khabakhpashev, and L. Shekhtman, "A low-dose x-ray imaging device," *European Journal Of Physics*, Vol. 19, no. 6, p. 475, 1998.

47. Mooney, R., and P. Thomas, "Dose reduction in a paediatric x-ray department following optimization of radiographic technique.," *The British Journal Of Radiology*, Vol. 71, no. 848, pp. 852–860, 1998.

48. Conway, B., P. Butler, J. Duff, T. Fewell, R. Gross, R. Jennings, G. Koustenis, J. McCrohan, F. Rueter, and C. Showalter, "Beam quality independent attenuation phantom for estimating patient exposure from x-ray automatic exposure controlled chest examinations," *Medical Physics*, Vol. 11, no. 6, pp. 827–832, 1984.

49. Harding, G., "X-ray scatter tomography for explosives detection," *Radiation Physics and Chemistry*, Vol. 71, no. 3-4, pp. 869–881, 2004.

50. Shaw, D., I. Crawshaw, and S. Rimmer, "Effects of tube potential and scatter rejection on image quality and effective dose in digital chest x-ray examination: An anthropomorphic phantom study," *Radiography*, Vol. 19, no. 4, pp. 321–325, 2013.

51. Don, S., R. MacDougall, K. Strauss, Q. T. Moore, M. J. Goske, M. Cohen, T. Herrmann, S. D. John, L. Noble, G. Morrison, *et al.*, "Image gently campaign back to basics initiative: ten steps to help manage radiation dose in pediatric digital radiography," *American Journal of Roentgenology*, Vol. 200, no. 5, pp. W431–W436, 2013.

52. Kaplan, S. L., D. Magill, M. A. Felice, R. Xiao, S. Ali, and X. Zhu, "Female gonadal shielding with automatic exposure control increases radiation risks," *Pediatric Radiology*, Vol. 48, no. 2, pp. 227–234, 2018.

53. Andriole, K. P., T. G. Ruckdeschel, M. J. Flynn, N. J. Hangiandreou, A. K. Jones, E. Krupinski, J. A. Seibert, S. J. Shepard, A. Walz-Flannigan, T. A. Mian, *et al.*, "Acr–aapm–siim practice guideline for digital radiography," *Journal of Digital Imaging*, Vol. 26, no. 1, pp. 26–37, 2013.

54. Food, D. Administration, *et al.*, "Fda report on the quality, safety, and effectiveness of servicing medical devices," 2018.

55. Goldman, J. M., "Solving the interoperability challenge: Safe and reliable information exchange requires more from product designers.," *IEEE Pulse*, Vol. 5, no. 6, pp. 37–39, 2014.

56. Kühn, F., and M. Leucker, "Or. net: Safe interconnection of medical devices," in *International Symposium on Foundations of Health Informatics Engineering and Systems*, pp. 188–198, Springer, 2013.

57. Altenstetter, C., "Medical device regulation in the european union, japan and the united states. commonalities, differences and challenges," *Innovation: The European Journal of Social Science Research*, Vol. 25, no. 4, pp. 362–388, 2012.

58. Weininger, S., M. B. Jaffe, M. Robkin, T. Rausch, D. Arney, and J. M. Goldman, "The importance of state and context in safe interoperable medical systems," *IEEE Journal Of Translational Engineering In Health and Medicine*, Vol. 4, pp. 1–10, 2016.

59. Tolk, A., S. Y. Diallo, and C. D. Turnitsa, "Applying the levels of conceptual interoperability model in support of integratability, interoperability, and composability for system-of-systems engineering," *Journal of Systems, Cybernetics, and Informatics*, Vol. 5, no. 5, 2007.

60. Robkin, M., S. Weininger, B. Preciado, and J. Goldman, "Levels of conceptual interoperability model for healthcare framework for safe medical device interoperability," in *2015 IEEE Symposium On Product Compliance Engineering (ISPCE)*, pp. 1–8, IEEE, 2015.

61. Goldman, J. M., S. Whitehead, S. Weininger, and M. Rockville, "Eliciting clinical requirements for the medical device plug-and-play (md pnp) interoperability program," *Anesthesia & Analgesia*, Vol. 102, pp. S1–54, 2006.

62. Medical Device Plug-and Play Interoperability Lab, M. G. H., "Medical device;plug-and-play; interoperability program," 2019.

63. Environment., O.S.I.C., "Openice - open-source integrated clinical environment.," 2019.

64. OR.NET, "Or.net e.v. â safe, secure and dynamic networking in the or.," 2019.

65. Kasparick, M., S. Schlichting, F. Golatowski, and D. Timmermann, "New ieee 11073 standards for interoperable, networked point-of-care medical devices," in *2015 37th Annual International Conference of the IEEE Engineering in Medicine and Biology Society (EMBC)*, pp. 1721–1724, IEEE, 2015.

66. Goldman, J. M., "Medical devices and medical systems-essential safety requirements for equipment comprising the patient-centric integrated clinical environment (ice)-part 1: General requirements and conceptual model," *ASTM International*, 2008.

67. Whitehead, S. F., and J. M. Goldman, "Hospitals issue call for action on medical device interoperability," *Patient Safety & Quality Healthcare*, Vol. 6, no. 1, p. 3, 2009.

68. Rhoads, J. G., T. Cooper, K. Fuchs, P. Schluter, and R. P. Zambuto, "Medical device interoperability and the integrating the healthcare enterprise (ihe) initiative," *Biomed Instrum Technol*, no. Suppl, pp. 21–27, 2010.

69. Logan, M., and B. Patel, "Medical device interoperability-a safer path forward," *AAMI, Arlington, VA2012*, 2012.

70. Vom, J., and I. Williams, "Justification of radiographic examinations: What are the key issues?," *Journal Of Medical Radiation Sciences*, Vol. 64, no. 3, pp. 212–219, 2017.

71. ANSI, The address of the publisher, *HL7 Reference Information Model ANSI/HL7 V3 RIM, R1-2003*, v3 ed., 2003.

72. Goldman, J. M., "Medical device connectivity for improving safety and efficiency," *American Society of Anesthesiologists Newsletter*, Vol. 70, no. 5, p. 5, 2006.

73. BRUSAN, A., "Syncbox." https://github.com/altaybrusan/syncbox, 2019.

74. Boffard, K. D., J. Goosen, F. Plani, E. Degiannis, and H. Potgieter, "The use of low dosage x-ray (lodox/statscan) in major trauma: comparison between low dose x-ray and conventional x-ray techniques," *Journal of Trauma and Acute Care Surgery*, Vol. 60, no. 6, pp. 1175–1183, 2006.

75. Deyle, S., A. Wagner, L. M. Benneker, V. Jeger, S. Eggli, H. M. Bonel, H. Zimmermann, and A. K. Exadaktylos, "Could full-body digital x-ray (lodox-statscan) screening in trauma challenge conventional radiography?," *Journal of Trauma and Acute Care Surgery*, Vol. 66, no. 2, pp. 418–422, 2009.

76. Giomataris, Y., P. Rebourgeard, J. P. Robert, and G. Charpak, "Micromegas: a high-granularity position-sensitive gaseous detector for high particle-flux environments," *Nuclear Instruments and Methods in Physics Research Section A: Accelerators, Spectrometers, Detectors and Associated Equipment*, Vol. 376, no. 1, pp. 29–35, 1996.

77. Venkatasubramanian, K., S. Gupta, R. Jetley, and P. Jones, "Interoperable medical devices," *IEEE Pulse*, Vol. 1, no. 2, pp. 16–27, 2010.

78. Lesh, K., S. Weininger, J. M. Goldman, B. Wilson, and G. Himes, "Medical device interoperability-assessing the environment," in *2007 Joint Workshop on High Confidence Medical Devices, Software, and Systems and Medical Device Plug-and-Play Interoperability (HCMDSS-MDPnP 2007)*, pp. 3–12, IEEE, 2007.

79. Larson, B. R., Y. Zhang, S. C. Barrett, J. Hatcliff, and P. L. Jones, "Enabling safe interoperation by medical device virtual integration," *IEEE Design & Test*, Vol. 32, no. 5, pp. 74–88, 2015.

80. Niezen, G., P. Eslambolchilar, and H. Thimbleby, "Open-source hardware for medical devices," *BMJ innovations*, Vol. 2, no. 2, pp. 78–83, 2016.

81. Samaras, E. A., and G. M. Samaras, "Confronting systemic challenges in interoperable medical device safety, security & usability.," *Journal of Biomedical Informatics*, Vol. 63, pp. 226–234, 2016.

82. Weininger, S., "Integrated clinical environment device model: Stakeholders and high level requirements," *Proc. Med. Cyber Phys. Syst., Seattle, WA, USA*, 2015.

83. Acosta, R., *et al.*, *Open source hardware*. PhD thesis, Massachusetts Institute of Technology, 2009.

84. MD, J. D. H., "Or.net e.v. a safe, secure and dynamic networking in the or.," 2011.

85. Chen, Z., A. Deguet, R. Taylor, S. DiMaio, G. Fischer, and P. Kazanzides, "An open-source hardware and software platform for telesurgical robotics research," in *Proceedings Of The MICCAI Workshop On Systems And Architecture For Computer Assisted Interventions, Nagoya, Japan*, Vol. 2226, 2013.

86. Purdon, P. L., H. Millan, P. L. Fuller, and G. Bonmassar, "An open-source hardware and software system for acquisition and real-time processing of electrophysiology during high field mri," *Journal of Neuroscience Methods*, Vol. 175, no. 2, pp. 165–186, 2008.

87. Beningfield, S., H. Potgieter, A. Nicol, S. Van As, G. Bowie, E. Hering, and E. Lätti, "Report on a new type of trauma full-body digital x-ray machine," *Emergency Radiology*, Vol. 10, no. 1, pp. 23–29, 2003.

88. Evangelopoulos, D. S., S. Deyle, H. Zimmermann, and A. K. Exadaktylos, "Personal experience with whole-body, low-dosage, digital x-ray scanning (lodox-statscan) in trauma," *Scandinavian Journal Of Trauma, Resuscitation and Emergency Medicine*, Vol. 17, no. 1, pp. 1–5, 2009.

89. Laskey, M., K. Lyttle, M. Flaxman, and R. Barber, "The influence o f t issue d epth and composition on the performance of the lunar dual-energy x-ray absorptiometer whole-body scanning mode.," *European Journal of Clinical Nutrition*, Vol. 46, no. 1, pp. 39–45, 1992.

90. Gershman, R. J., R. E. Cabral, N. Berger, and J. A. Stein, "Whole-body x-ray bone densitometry using a narrow-angle fan beam, including variable fan beam displacement between scan passes," Nov. 17 1998. US Patent 5,838,765.

91. Luo, T. D., A. A. Stans, B. A. Schueler, and A. N. Larson, "Cumulative radiation exposure with EOS imaging compared with standard spine radiographs," *Spine Deformity*, Vol. 3, no. 2, pp. 144–150, 2015.

92. Bittersohl, B., J. Freitas, D. Zaps, M. R. Schmitz, J. D. Bomar, A. R. Muhamad, and H. S. Hosalkar, "EOS imaging of the human pelvis: reliability, validity, and controlled comparison with radiography," *JBJS*, Vol. 95, no. 9, p. e58, 2013.

93. Schatzki, T., R. Haff, R. Young, I. Can, L. Le, and N. Toyofuku, "Defect detection in apples by means of x-ray imaging," *Transactions of the ASAE*, Vol. 40, no. 5, pp. 1407–1415, 1997.

94. Hu, L., and R. Desjardins, "Non-destructive evaluation of finger-joint strength using an on-line x-ray scanner," *World Conference on Timber Engineering*, 2010.

95. Evangelopoulos, D., M. von Tobel, D. Cholewa, R. Wolf, A. K. Exadaktylos, and Z. Zachariou, "Impact of lodox statscan on radiation dose and screening time in paediatric trauma patients," *European Journal Of Pediatric Surgery*, Vol. 20, no. 06, pp. 382–386, 2010.

96. Durmaz, F. A., A. Brusan, and C. Ozturk, "Unified open hardware platform for digital x-ray devices; its conceptual model and first implementation," *IEEE Journal of Translational Engineering in Health and Medicine*, 2020.

97. Dorf, R. C., and R. H. Bishop, "Modern Control Systems," *Pearson Addison-Wesley*, 1998.